

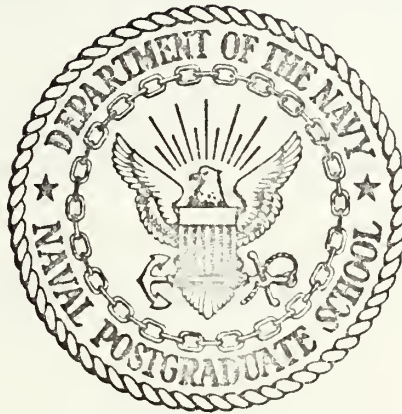
THE DESIGN AND DEVELOPMENT OF A NON-  
FLAPPING ROTOR SYSTEM UTILIZING INFLEXIBLE  
BLADES AND EMPLOYING A NEW ROTOR CONTROL  
MECHANISM

William Alfred Simmons

Library  
Naval Postgraduate School  
Monterey, California 93946

# NAVAL POSTGRADUATE SCHOOL

## Monterey, California



# THESIS

THE DESIGN AND DEVELOPMENT OF A NON-  
FLAPPING ROTOR SYSTEM UTILIZING INFLEXIBLE  
BLADES AND EMPLOYING A NEW ROTOR CONTROL  
MECHANISM

by

William Alfred Simmons

Thesis Advisor:

J. A. J. Bennett

December 1972

Approved for public release; distribution unlimited.

Library  
Naval Postgraduate School  
Monterey, California 93940

The Design and Development of a Non-Flapping Rotor  
System Utilizing Inflexible Blades and  
Employing a New Rotor Control Mechanism

by

William Alfred Simmons  
Lieutenant, United States Navy  
B.S., United States Naval Academy, 1966

Submitted in partial fulfillment of the  
requirements for the degree of

AERONAUTICAL ENGINEER

from the

NAVAL POSTGRADUATE SCHOOL  
December 1972



## ABSTRACT

The intent of this study was the design, development and preliminary testing of an inflexible blade, hingeless rotor system. A hingeless system was desired due to its advantage of augmented control power resulting from its ability to transfer bending moments across the hub. The inflexible blades offered the unconventional feature of reducing the magnitude of blade flap-wise flexing to substantially zero and of removing the resultant problems of rotor dynamics. These stiffer blades generally dictated the use of more compact rotors, i.e., of a smaller diameter and therefore of a higher disk loading. The control rotor was of unconventional design and utilized a relatively small, free-flapping rotor to convey cyclic commands to the main rotor blades and provide rolling trim with varying forward speed. The present study has yielded a simple, mechanical system that essentially satisfies the design criteria and shows sufficient promise to warrant further development and testing.





## TABLE OF CONTENTS

I.	INTRODUCTION-----	7
II.	BACKGROUND AND DEVELOPMENT-----	8
III.	ROTOR HEAD DESIGN GENESIS-----	11
	A. FREE-FLAPPING ROTOR HEAD DESIGN-----	11
	B. FULL-FEATHERING ROTOR HEAD DESIGN-----	13
IV.	TESTING AND DESIGN MODIFICATIONS-----	24
	A. FREE-FLAPPING ROTOR AND MODEL TESTS-----	24
	B. INITIAL FULL-FEATHERING ROTOR HEAD TESTS--	32
	C. REDESIGN AND SUBSEQUENT TESTS-----	34
	D. FURTHER ALTERATIONS AND TESTS-----	34
V.	DESIGN FEASIBILITY DISCUSSION-----	39
VI.	CONCLUSIONS-----	41
APPENDIX A	LIFT MOMENT DISSYMMETRY-----	43
APPENDIX B	WIND TUNNEL AND AIRSPEED MEASUREMENT SYSTEM-----	49
APPENDIX C	ROTOR TEST PYLON-----	52
APPENDIX D	FINAL HEAD DRAWINGS AND PHOTOGRAPHS-----	56
	BIBLIOGRAPHY-----	69
	INITIAL DISTRIBUTION LIST-----	70
	FORM DD 1473-----	71



## LIST OF FIGURES

<u>FIGURE</u>	<u>TITLE</u>	
III-1	Free-Flapping Rotor Components-----	12
III-2	Rotor Blade Construction-----	12
III-3	New Head Basic Operation Model-----	15
III-4	Initial Inner Control Rotor Plate Mechanisms--	16
III-5	Final Inner Control Rotor Plate Mechanisms----	19
III-6	Main Rotor Head Core Element-----	20
III-7	Control Rotor Base Plate-----	20
III-8	Main Blade Attachment Unit-----	21
III-9	Reversing Link Base Plate-----	22
III-10	Views of Assembled Head-----	23
IV-1	Table of Lift for Free-Flapping Rotor Tests---	30
IV-2	Rotor Starting Drum-----	31
IV-3	Two Views of the Final Model Version-----	31
IV-4	Head Junction Block-----	36
IV-5	Hydraulic Vibration Dampers-----	37
IV-6	Table of New Rotor Head Performance Data-----	38
A1	Blade Velocity Distribution-----	43
A2	Example Velocity Distribution-----	45
B1	Naval Postgraduate School Smoke Tunnel-----	49
B2	Smoke Tunnel Test Equipment-----	51
C1	Two Views of the Rotor Test Pylon-----	53
C2	Strain Gage Bridge and Trim System-----	54
C3	Test Pylon with Full-Feathering Head-----	55
D1	Free-Flapping Rotor Base Plate-----	57



D2	Base Plate Pivot Block-----	58
D3	Reversing Link Base Plate-----	58
D4	Main Rotor Head Core Element-----	59
D5	Control Rotor Base Plate-----	59
D6	Main Blade Attachment Unit-----	60
D7	Assembled Rotor Head-----	61
D8	Two Views of Mounted Rotor Head-----	64
D9	Two Views of Mounted Rotor Head-----	65
D10	Two Views of Mounted Rotor Head-----	66
D11	Two Views of Mounted Rotor Head-----	67
D12	Two Views of Rotor Test Set-Up-----	68



## ACKNOWLEDGEMENTS

I would like to acknowledge the help and inspiration of Professor J. A. J. Bennett and Lt. R. A. Wiley, USN, who together, have provided the means and incentive to study rotary-winged flight and to undertake this project.





## I. INTRODUCTION

Contemporary rotor heads, for the most part, utilize a blade arrangement in which each blade is hinged at the root end thus allowing the blade freedom of motion in the flapping sense. The main purpose of this flapping freedom is to balance the lateral moment of rotor lift. Although the flapping hinge provides one solution to the lift moment dissymmetry problem, it introduces a number of problems of its own.

The flapping hinge is normally very inefficient due to the use of a 360° bearing-type of surface which provides the freedom of the few degrees that are necessary. This hinge and its associated hardware are quite costly in terms of weight, complexity, maintenance and added construction costs due to the increased number of parts required. An important limitation of a rotor system employing centrally located flapping hinges is that control is dependent on rotor thrust which gives zero control in the absence of thrust, e.g., when landing in autorotation.

The flapping hinge, for the above reasons, is a somewhat crude solution to the problem. Since flapping is merely effective feathering and most rotors already employ a feathering hinge to provide collective control, a more logical solution would be to feather the blades cyclically and eliminate the flapping hinge entirely. This was the approach taken for the design feasibility study presented herein.



## II. BACKGROUND AND DEVELOPMENT

In the early 1920's Juan de la Cierva delved into the realm of rotary-wing flight to find a solution to the airplane's poor slow-speed handling characteristics, mainly the stall. He developed the autorotation principle and then applied this concept to a rotorcraft embodying an aircraft fuselage and a lifting rotor. During his early tests he found that the machine tended to roll over as forward speed was gained during the take-off run, the rolling being due to the lift moment dissymmetry produced by the forward motion (see APPENDIX A). His solution to this problem was to give each blade an additional degree of freedom, i.e., that of flapping motion about a hinge at the blade root. The flapping hinge eliminated the transmission of rolling or lift moments to the fuselage.

With the provision of a flapping hinge, the blade coning angle (the non-periodic component of flapping) was determined by a balance of the blade lifting and centrifugal moments. As the blades were hinged substantially on the axis of rotation, the lift forces were transmitted to the hub with virtually no accompanying moments. Cierva's early machines employed an auxiliary fixed wing with ailerons to provide lateral control, the rotor providing lift but not control. In his later machines, Cierva eliminated the wing and mounted the rotor on a gimbaled joint which, by allowing the rotor hub to be tilted, achieved direct control independent of



forward speed. This control was dependent on thrust and, more specifically, was proportional to the product of the rotor thrust and the distance this thrust vector was displaced from the CG of the aircraft.

The flapping hinge subsequently underwent many refinements and alterations. Two of the more important variants were the "alpha-two" and "delta-three" hinges. The  $\alpha_2$  hinge allowed the elimination of mechanical damping without a tendency towards ground resonance. This hinge coupled flapping motion with drag motion without appreciable pitch change for small displacements. The  $\delta_3$  hinge was used to give a feathering displacement when the blade was displaced in the flapwise sense and, consequently, reduced the magnitude of this flapping. Even though these hinges served very useful purposes, the rotor itself was still limited by the fact that control was dependent on the tilt of the tip-path plane and the thrust produced.

The approaches of the Bell and Hiller companies to the flapping problem, although employing different control mechanisms, were somewhat similar in that they both used a centrally-pivoted two-bladed rotor. These rotor types have been termed "semi-rigid" as there is no coning freedom. However, they do not transmit lift moments to the aircraft itself as the tip-path plane has complete freedom to tilt about the common flapping hinge. These rotor arrangements work quite well but are limited to smaller vehicles by the inherent vibration of two-bladed rotors. The smaller-sized



inflexible rotor is, however, the one with which this present study deals. Consequently, a conventional two-bladed rotor with inflexible blades is used for comparison.

With the goal of achieving better control characteristics, the recent trend has been towards systems that can take bending moments across the hub and transmit them to the aircraft. Two such systems currently under development are the Lockheed "rigid rotor" and the Sikorsky offset flapping-hinge systems. Lockheed's "rigid rotor" system (obviously a misnomer) utilizes relatively flexible blades which effectively assume the role of the flapping hinge. Sikorsky, being somewhat more conservative in nature, has merely moved the flapping hinges outboard to around 12-15 percent of the blade radius. Both methods produce the desired results but, while one retains the flapping hinge hardware, the other introduces the dynamic problems of flexible blades.

This recent trend, in effect, is a relapse towards the original problem of hingless blades, but lift moments across the hub are now controlled by cyclic pitch change, i.e., by sinusoidal feathering. A purpose of this study was to return to the original problem and approach it from a pure feathering viewpoint. A fresh outlook could thus be gained by studying a rotor in which flapping substantially is eliminated and is replaced entirely by feathering. To reiterate once again, the features that made feathering desirable were augmented control power, control independent of rotor thrust, stabilized control response and elimination of the flapping hinge and associated hardware.





### III. ROTOR HEAD DESIGN GENESIS

Two basic rotor head designs were investigated in this study. The first was a simple, free-flapping rotor, the features of which were then incorporated into the second design, a full-feathering system utilizing a free-flapping control rotor.

#### A. FREE-FLAPPING ROTOR HEAD DESIGN

In order to get a feel for the dynamics and properties of smaller, model-sized rotors, a very simple two-bladed "teeter-totter" rotor was designed and built. The basic parts of this head are shown in FIG. III-1 and were joined together with a 1/4-inch aircraft bolt. The rotor blades were constructed using 3/4-by 3/8-inch pieces of fir for the leading edges and 3/8-by 1 1/2-inch formed balsa trailing edge pieces. These were glued together, planed and sanded to an airfoil section. The blades then had 1/16-inch plywood reinforcing plates added to the root-end upper and lower surfaces and finally were covered with silk and dope. The blades were symmetrical in section with a chord of 2 1/4 inches and a radius of 20 7/8 inches (giving a total rotor diameter of 42 7/8 inches when mounted on the rotor base plate). Each blade also had roughly 2° of dihedral and 2° of positive incidence built into it (relative to the lower plywood reinforcing plate). Figure III-2 shows the blades during construction.



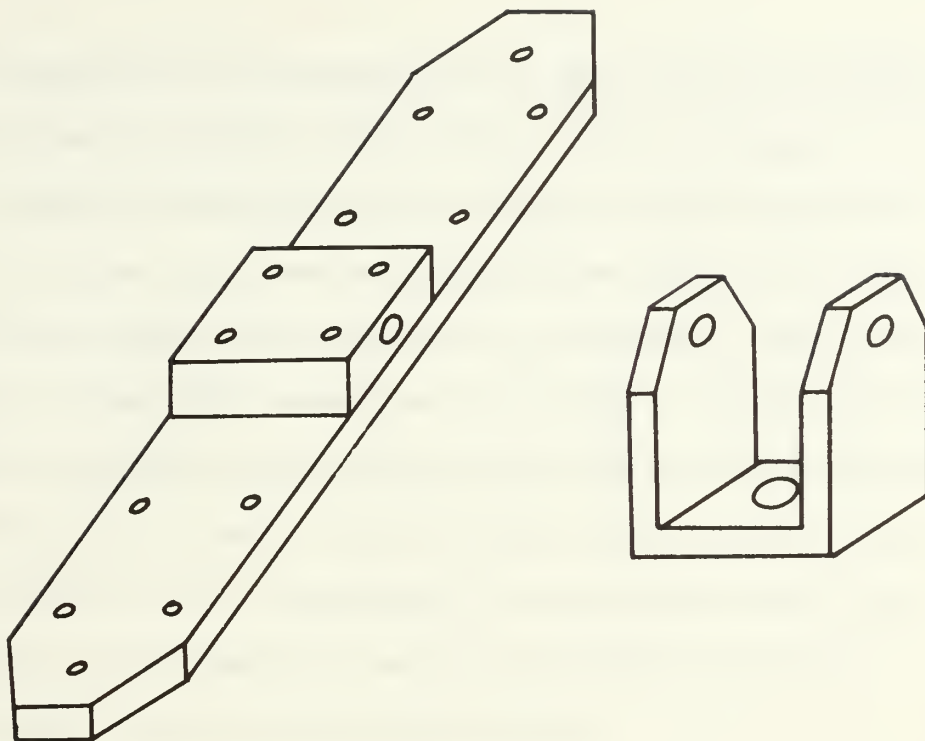


FIGURE III-1 Free-Flapping Rotor Components

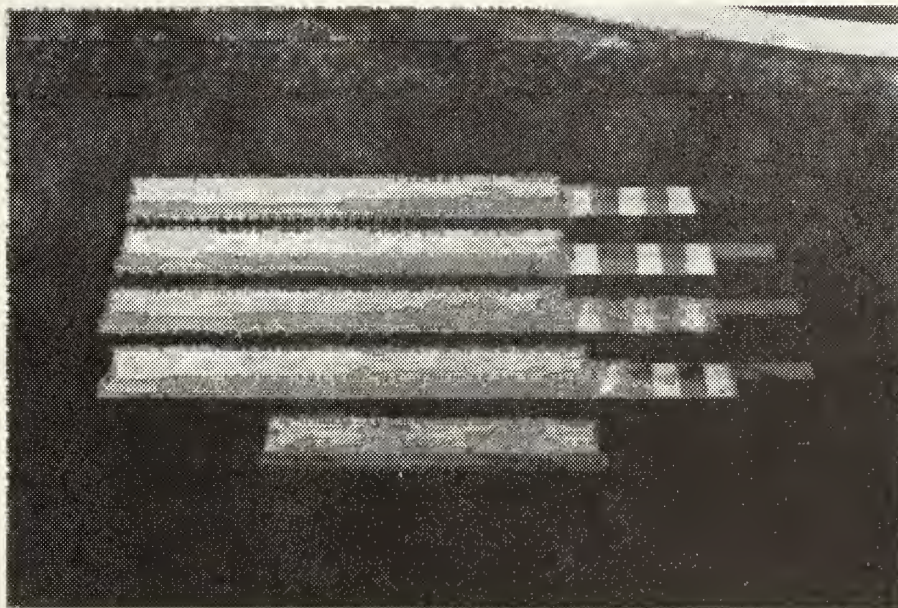


FIGURE III-2 Rotor Blade Construction



The construction and testing of this rotor provided a baseline against which future tests of more complex rotor systems could be compared with respect to the required angles of attack for, and representative RPM's of, autorotation and model rotor dynamics in general. The early testing of this rotor was done by mounting the rotor bearing hub to the bottom of an old pan and holding the pan above a car (with the top down) while driving down a road. This worked quite well for preliminary testing and gave the approximate rotor angle of attack and blade incidence combinations required for autorotation.

It was found that the incidence angle had to be reduced to approximately  $0^\circ$  (as opposed to the  $+4^\circ$  to  $+5^\circ$  incidence normally used with full-sized machines) and shims were fitted to accomplish this reduction. The best rotor angle of attack appeared to be roughly  $15-20^\circ$  once autorotation was fully developed. The knowledge gained from this rotor was then applied to the design of the full-feathering rotor head.

#### B. FULL-FEATHERING ROTOR HEAD DESIGN

As previously stated, the goal of this project was to design a simple, mechanical system that would provide lateral trim with varying forward speed. Returning to the original problem of lift moment dissymmetry with forward speed, a solution was sought that would allow the main rotor blades to feather cyclically (as opposed to flapping freely) in order to balance this dissymmetry. The experience gained from the





free-flapping, teeter-totter rotor suggested that such a rotor might be used for feathering, i.e., to control the pitch angle of the main rotor blades.

With a free-flapping rotor, a  $90^\circ$  control advance is required, but theoretically this control advance reduces to zero for a completely stiff (inflexible) and rigidly mounted blade. This fact was utilized and allowed the use of two rotors (control and main) set apart by  $90^\circ$ . Any control input would precess the control rotor and become effective  $90^\circ$  later as the main blade reached the position of control input. The control rotor, being mechanically coupled to the main blades, would then feather the main blades to achieve the desired control. This arrangement worked very similarly to the Hiller rotor control system with the exception that the main blades now had augmented flapping stiffness. These initial ideas were drawn to get a feeling for the required mechanical system.

The problem of transmitting cyclic control was solved first. A take-off from the "leading" side of the hinged control rotor plate (FIG. III-3) was linked to an arm extending forward above the main rotor blade and controlling the main blade pitch (feather) angle. The two control rotor paddles were mechanically linked together and decreased the pitch of one as the pitch was increased on the other. Control inputs in the form of pitch changes to the control rotor paddles were initiated as the control rotor was aligned in the direction of the desired control. This produced opposed





incremental changes in the lift of the two paddles due to the change of the pitch angle and hence angle of attack. Therefore, 90° later, the control rotor would be displaced, flapwise, in the sense of control input. The displacement was transmitted to the main blade control arms and produced an opposed change in pitch of the main rotor blades. This, in turn, produced an opposed incremental lift of the main blades, i.e., a rolling (control) moment in the desired direction. The control moment was transferred directly to the hub (through the use of hingeless blades) and thus to the fuselage.

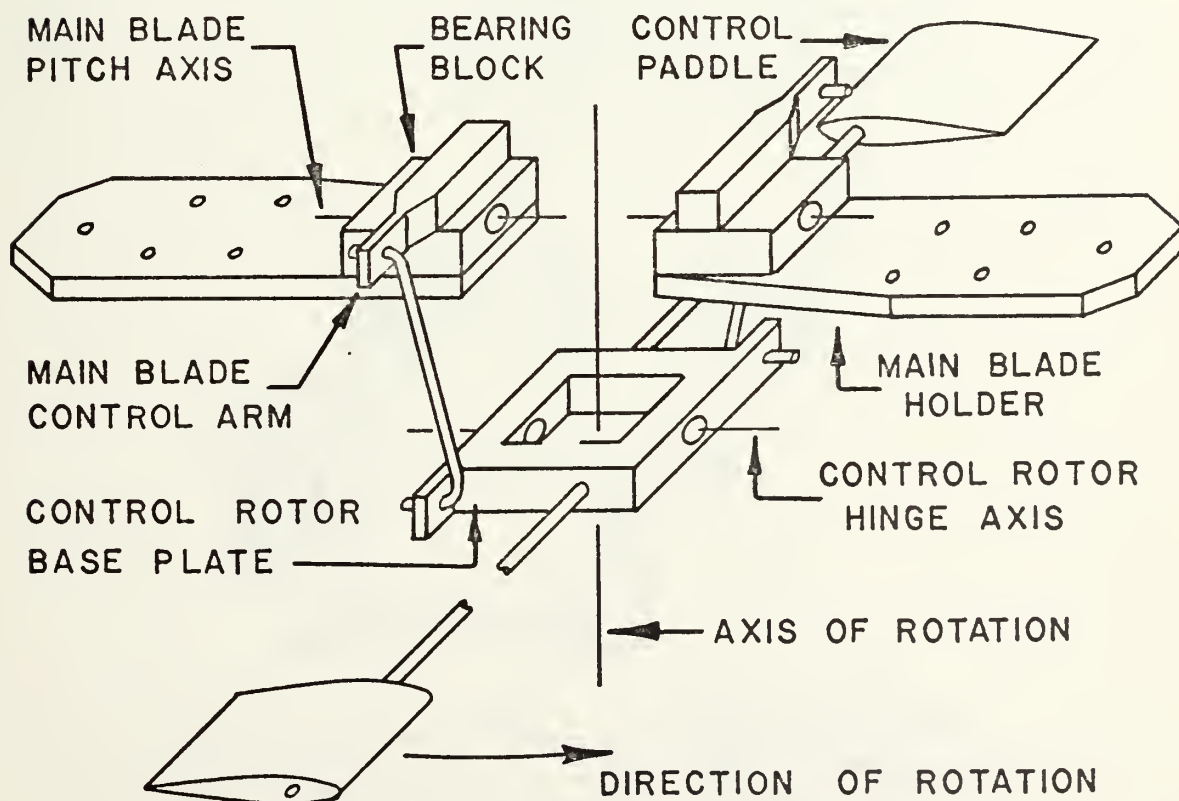


FIGURE III-3 New Head Basic Operation Model



Incorporation of a collective pitch mechanism was undertaken next. The requirement was to increase or decrease the pitch of both main blades simultaneously and independently of cyclic control action. The control rotor plate was modified to incorporate the linkage arrangement as shown in FIG. III-4. The collective control was entered at the pivot point of the control rotor plate thereby divorcing the collective input from the control rotor flapping. In FIG. III-4, it can be seen that an upwards collective input will give a decrease in collective pitch and vice versa. Two main problems were encountered with this arrangement.

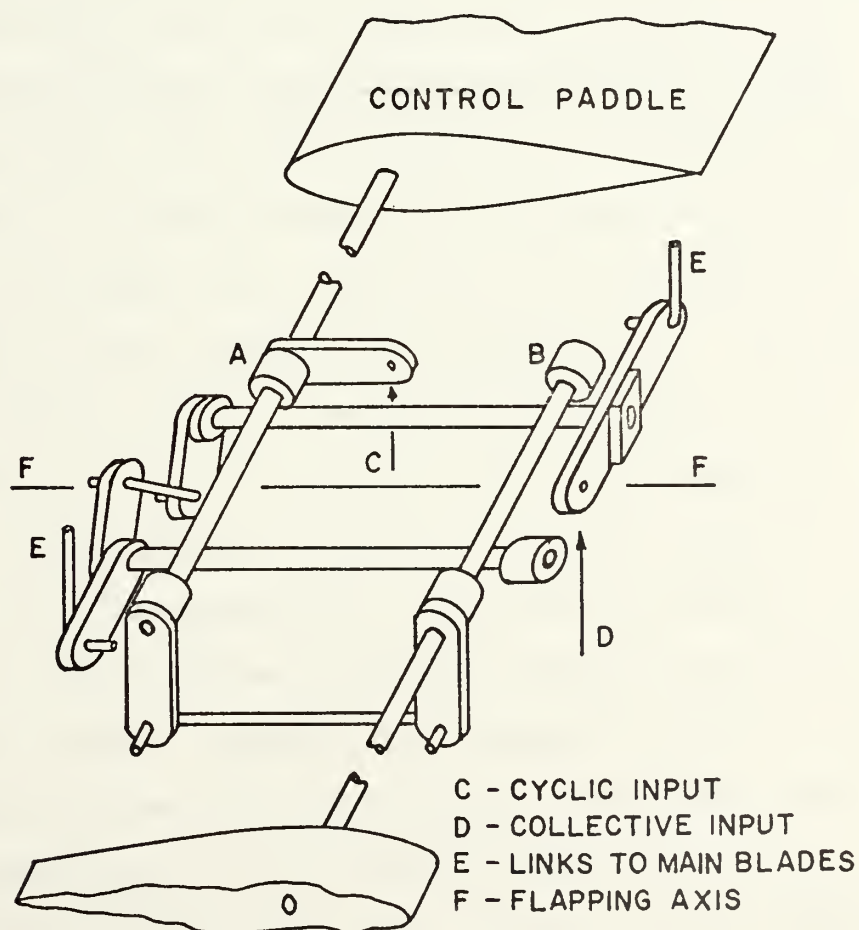


FIGURE III-4 Initial Inner Control Rotor Plate Mechanisms



Firstly, due to the location of the cyclic control input, it was noted that the cyclic control was not independent of control rotor flapping. If, say, the cyclic control arm was pulled to increase the pitch angle of the nearest paddle, the resultant flapping would further increase the pitch angle. Furthermore, shifting the attachment point of the cyclic control arm to point B from point A (FIG. III-4) did little to help matters. The resultant flapping then tended to negate the control input altogether. This problem was, however, far overshadowed by the second problem.

The second problem area was one of the primary functions that the control rotor was supposed to fulfill, i.e., that of providing lateral trim with varying forward speed. To accomplish this, the control rotor was supposed to sense the difference in velocity between the paddles at the  $\psi=90^\circ$  and  $\psi=270^\circ$  positions and then convert this velocity difference to a cyclic pitch command to the main rotor. The advancing control paddle ( $\psi=90^\circ$ ) would see a velocity of  $\omega R + V$  as compared to a velocity of  $\omega R - V$  for the retreating ( $\psi=270^\circ$ ) paddle. In actuality, assuming a positive rotor angle of attack (as in autorotation), the advancing paddle would produce more lift than the retreating paddle and would flap (precess) upwards, reaching the summit  $90^\circ$  later ( $\psi=180^\circ$ ). This would increase the pitch angle of the main rotor blade which would then be at the  $\psi=90^\circ$  position. In other words, the advancing blade would see a higher velocity and be at a



higher angle of attack. This would produce a strong difference in lift (and therefore lateral rolling moment) instead of a reduced angle of attack in order to balance the moment to zero at the hub. Thus the control system was working in reverse.

Machine work had been completed on some of the major pieces thus making a total redesign impractical. Therefore, a modification was designed that would incorporate small reversing links and an attachment plate to integrate the reversing links with the main rotor head member. While these parts were being drawn and built, the cyclic control/flapping problem was solved. The cyclic control input, like the collective control input, was rerouted to the control rotor flapping hinge line, making the cyclic control inputs virtually independent of control rotor flapping.

The revised linkage arrangement within the control rotor plate, along with the reversing links (which are attached to the main hub member and do not flap with the control rotor), are shown in FIG. III-5. The main blade control arms (FIG. III-3) were also reversed and linked behind the main blade holders instead of in front of the holders as before. The control arms, now facing aft, were linked to the output of the reversing links ("E" - Fig. III-5).

The final arrangement did, in fact, satisfy the design goals of three independent inputs to the main rotor blades, i.e., cyclic control, collective control and lateral trim with varying forward speed. The collective control was





essentially unaltered from the earlier version. The cyclic control worked similarly with two exceptions. First, it now lagged 90° behind the main blade that it directly controlled instead of leading it by 90°, and second, cyclic control was now independent of control rotor flapping. The lateral trim also worked in the proper sense and feathered the lagging main blade to a lower pitch angle as the control rotor flapped upwards, and vice versa.

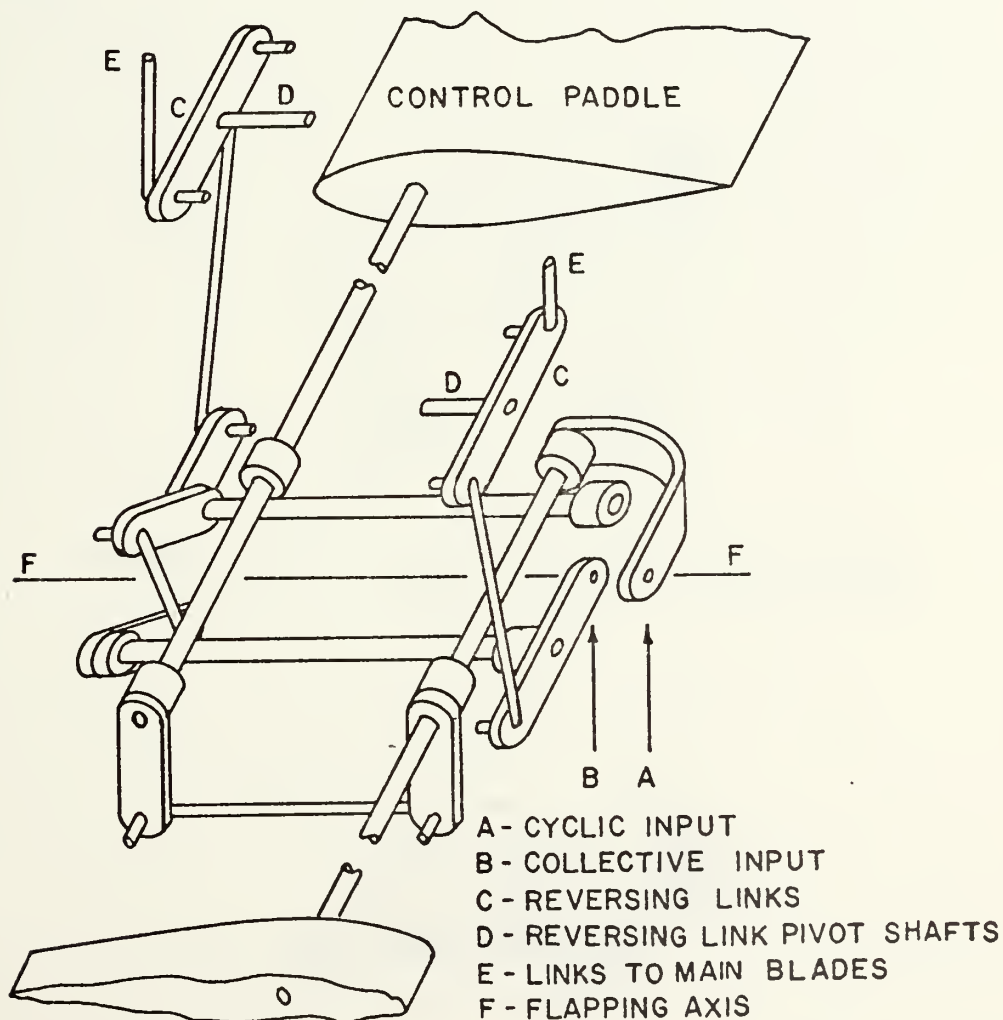


FIGURE III-5 Final Inner Control Rotor Plate Mechanisms



The finalized design was then assembled. The central element of the entire unit was the rotor head core shown in FIG. III-6. Most of the other elements were attached to the main core which, in turn, was the attachment point to the main rotor shaft for the whole head assembly. The control rotor base plate is shown in FIG. III-7 and is the housing for most of the mechanisms shown in FIG. III-5 as previously explained. The control rotor was attached to the core with two 3/16-inch pins which allow the plate to have flapping freedom.

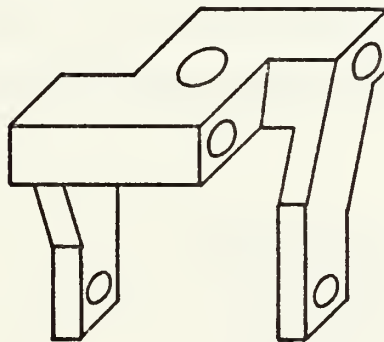


FIGURE III-6 Main Rotor Head Core Element

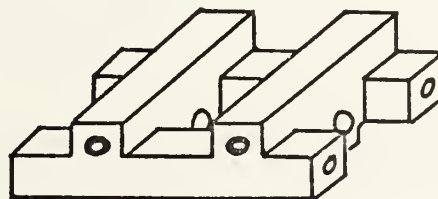


FIGURE III-7 Control Rotor Base Plate



The main blade attachment units are shown in FIG. III-8. Each unit was comprised of a blade attachment plate, unit bearing block and blade pitch control arm. The two units were attached to the core element with 1/4-inch aircraft bolts which formed the main blade feathering (pitch) axes. The bolts were fixed relative to the core element, and the blade attachment units rotated with respect to the bolts and core element. The blade attachment units were designed such that the unit pitching axes, formed by the 1/4-inch bolts, were coincident with the main blade quarter-chord lines, i.e., the blade aerodynamic neutral axes. Just outboard of the unit bearing blocks, the attachment plates were recessed to allow clearance for the bolt heads as the units rotated.

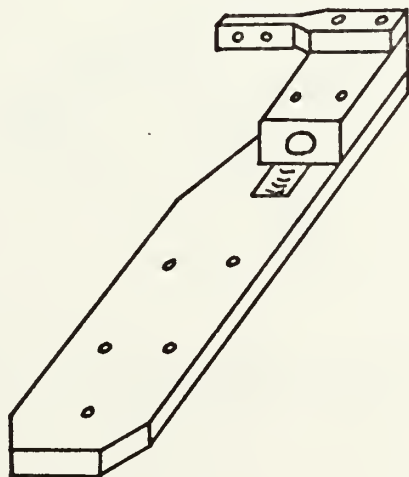


FIGURE III-8 Main Blade Attachment Unit



The reversing link base plate is shown in FIG. III-9. This plate rested immediately on top of the core element and was secured to it by the main rotor shaft retaining nut. The relative positioning of all of the main units along with the various linkage connections can be observed in FIG. III-10, and the detail drawings of all of the main rotor head pieces are included in Appendix D.

The machine work on the various parts contained in the two heads was done at the Aeronautics machine shop, Naval Postgraduate School, Monterey.

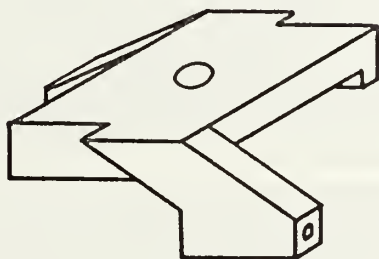


FIGURE III-9 Reversing Link Base Plate





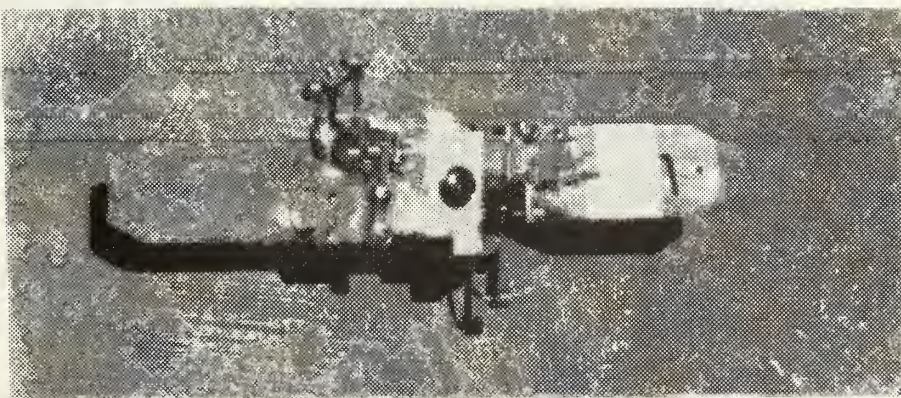
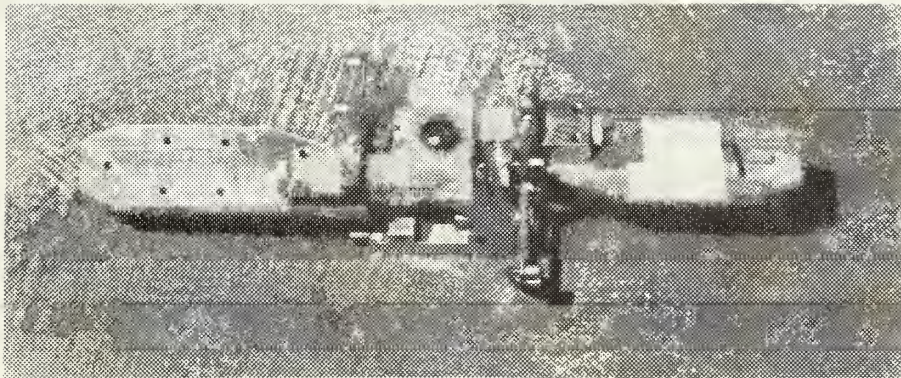
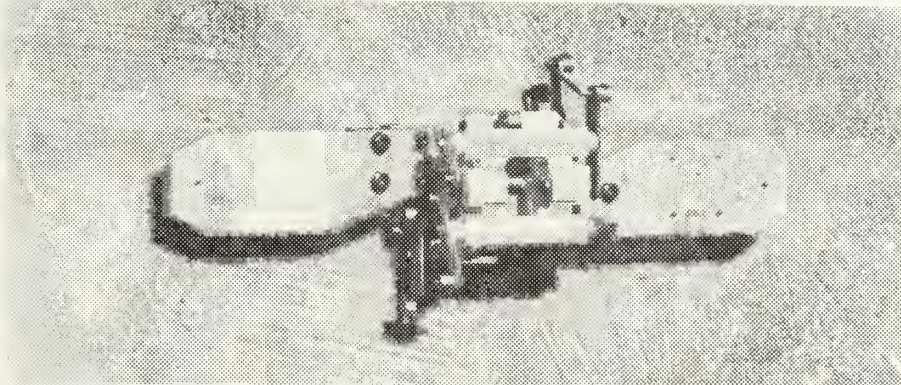
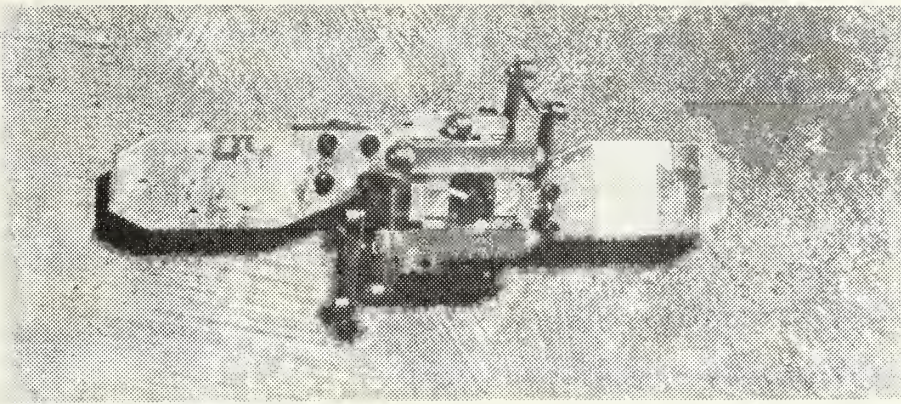


FIGURE III-10 Views of Assembled Lead





#### IV. TESTING AND DESIGN MODIFICATIONS

During the process of testing the rotor heads used in this project, three different means of testing were employed utilizing, respectively, a free-flying radio-controlled model, a moving platform (a car with the top down) and a low-speed wind tunnel (APPENDIX B).

##### A. FREE FLAPPING ROTOR AND MODEL TESTS

The initial plan was to do much of the experimental work on the rotor heads by mounting them on a model aircraft fuselage suitably modified to incorporate a rotor pylon. The plan was to fly the model by radio control (R/C) to investigate the rotor operating characteristics under actual flight conditions. The free-flapping rotor, therefore, was mounted on a servo-controlled, two-degrees-of-freedom gimbal to give tilt-head control as utilized on the later Cierva Autogiros. In addition to the two controls for the rotor head the model had controls for the engine throttle, a trimmable elevator and a rudder with steerable tailwheel.

The first attempts at flight were unsuccessful. The rotor was brought up to speed, as far as possible by hand, while the engine was run at full power. The model was then released to start its take-off run. The rotor was observed to slow down with an accompanying increase in the magnitude of blade flapping. Finally, the flapping would overpower the servo mountings, and the blades would strike the aft



fuselage halting all further rotation. Multiple runs were made with very consistent results. Before attempting further runs, it was decided to investigate the reasons for the rotor's failure to autorotate by working with the rotor without the rest of the model.

Subsequent testing was performed with the rotor mounted on the bottom of a pan and held above a car as mentioned earlier. This proved to be quite a simple and expeditious method of testing as virtually no preparation or test equipment was required. With the blades at their initial incidence angle of approximately  $+2^{\circ}$ , it was found that the rotor had to be held at a negative angle of attack for rotation to sustain the initial hand-started rotation. The positive blade angle originally had been selected since full-size machines autorotate at around a  $+5^{\circ}$  blade angle.

Prior to further testing, two sets of shims of  $3^{\circ}$  and  $6^{\circ}$  were made to fit between the rotor pivot plate and the blades. These reduced the blade angle to about  $-1^{\circ}$  and  $-4^{\circ}$  respectively. With the  $3^{\circ}$  shims in place, the rotor would autorotate consistently at a rotor angle of attack of approximately  $20-25^{\circ}$ . At forward speeds of 25 MPH, approximately 15-20 pounds of lift could be developed. Rotor acceleration from a fast hand-flip start to a steady autorotational speed (roughly from 800 to 1000 RPM) was accomplished in 10 to 15 seconds. With the  $6^{\circ}$  shims in place, the rotor would start much more easily and accelerate much more quickly (about 5 seconds). However, the final steady rotational speed was



considerably lower and much less lift was produced. The 3° shims were used, therefore, for the remaining test work.

While the rotor was being tested, the fuselage was modified to incorporate some of the lessons learned. A higher, wider landing gear was fabricated to increase the rotor angle of attack to approximately 20° during the take-off run. Also, the rotor pylon was raised 4 inches to allow the blades more flapping freedom without striking the fuselage. Flapping stops were also added to the rotor head to give additional insurance that the blades would remain clear of the fuselage.

Flying of the model was once again attempted after all of the modifications were completed. The rotor seemed on the verge of speeding up when the blades appeared to strike the fuselage once again. The second attempt produced similar results but also damaged the gimbal control servo mounts and linkages. Flight was then attempted with the rotor gimbals completely locked, i.e., with no head tilt possible. This time, with the system rigid enough to prevent the blades from striking the fuselage, the rotor accelerated and the model appeared to be almost ready to lift off when it rolled to the left striking the blades against the runway. Subsequent evaluation revealed that the lateral control power was insufficient to counteract the engine torque which then caused the roll as the weight was lifted from the wheels.

While the blades were being refurbished, the decision was made to perform some simple testing in the wind tunnel to





ensure that the model was fully controllable before further free flight (and the resultant repair and overhaul) was attempted. Due to the rolling problem, the lateral gimbal control was reactivated. In order to cope with the high forces produced when the rotor was hitting the flapping stops during initial acceleration, the lateral input was given a longer lever arm to work on. This reduced the control forces required of the servo although it did decrease the total lateral control available.

The model was mounted in the tunnel with wires leading from the propeller hub upstream to anchors in the tunnel walls (to simulate the propulsive force and maintain the model in position). The main landing gear was also tied to the tunnel floor allowing sufficient movement for the gear to rise off the floor but not enough to allow the rotor to strike the floor or walls. The radio gear was utilized allowing control of the lateral head tilt, elevator and rudder during tunnel operation.

The model flew quite well in the tunnel and displayed good lateral, longitudinal and directional control. The weight of the model was 5 pounds 4 ounces in the tunnel configuration (no fuel). At maximum tunnel velocity (22 MPH), the model would lift off at 1150 RPM (as measured with a General Radio Model 1540 STROBOLUME), produced 3 pounds of drag at lift-off, 2 pounds in level flight and 3 1/2 pounds at full load (full up elevator). Further tests indicated that the model would just lift with two additional pounds.



Finally, it was felt that a sufficient amount had been learned to attempt free flight once again. The take-off run went quite smoothly although the rotor accelerated quite slowly. Near the end of the run, the rotor could be seen to speed up quite quickly. Up elevator was being held to keep the tail on the ground and thus keep the rotor at a high angle of attack. When the aircraft finally did lift off, it literally jumped into the air, pitched up more than  $90^{\circ}$  and crashed. The crash was caused by a combination of poor pilot reaction and a misplaced center of gravity. The CG had been checked but had not been repositioned, considering how well the model had "flown" in the tunnel.

It was interesting to note that the tunnel tests had not indicated the ensuing problem. In retrospect, it was seen that the wires attaching the propeller hub to the tunnel walls changed the "thrust" vector enough to balance out the tail-heavy moment as it was generated. One of the limitations of tunnel testing was therefore vividly displayed. The fuselage was rebuilt to repair the damage, and the CG was moved to ensure that the rotor thrust vector passed through it (as it should have done before).

While the fuselage was being rebuilt, the rotor was removed and mounted on the rotor test pylon (APP. C) in the wind tunnel in order to investigate certain aspects of model rotor performance. The most efficient incidence and rotor



attack angles were sought along with the effects that these angles had on the relative lifts that could be produced by the rotor.

Due to the uncertain life expectancy of the rotor blades on the free-flying model, two new sets of rotor blades were made for subsequent tunnel testing. These blades were just under 22 inches long (giving a rotor diameter of 45 inches) with a chord of 2 1/4 inches, no dihedral and no built-in blade angle. The zero blade incidence angle was desired so that a more accurate value for the optimum incidence could be obtained using the shims.

Tests were run with the 3° and 6° shims (both positive and negative). It then appeared that the 6° shims were just too far afield. Therefore, the 6° shims were modified to 1 1/2° shims. The results of the final tests with the 1 1/2° and 3° shims (along with no shims) can be seen in the table in FIG. IV-1. The rotor speed varied from about 500 RPM (with the +3° shims at 10° rotor angle of attack) to about 1250 RPM (with the +1 1/2° shims at 35° rotor angle of attack).

As the fuselage once again neared readiness for further flight attempts, a means was devised to overcome the poor initial rotor acceleration during the take-off run. A four-inch drum was made and fitted just under the rotor on the rotor shaft (FIG. IV-2). A cord was wrapped around the drum a number of times, routed back along the fuselage and anchored to the ground. Then, as the model gained



translational speed, the cord would spin the rotor, the drum being so designed as to bring the rotor up to about 1000 RPM as the model accelerated to 10 MPH. This method had been used successfully on full-size autogyros for similar purposes. The final version of the model is shown in FIG. IV-3.

ROTOR ANGLE of ATTACK (DEGREES)	BLADE INCIDENCE ANGLE (DEGREES)				
	-3	-1 1/2	0	1 1/2	3
0	-	-	-	-	-
5	-	-	0.4	0.6	-
10	0.7	0.7	0.8	1.0	1.2
15	1.0	1.4	2.0	2.4	1.4
20	1.5	2.0	3.0	4.1	-
25	2.2	3.3	5.0	6.5	-
30	2.9	4.2	6.5	8.3	-
35	3.6	5.2	8.1	10.0	-

- Notes: 1) "-" indicates autorotation would not sustain itself  
 2) values in table are approx. pounds of lift  
 3) all values in the 1 1/2° column accelerated to speed very slowly, e.g., it took a full minute to reach the final value of 10.0

FIGURE IV-1 Table of Lift for Free-Flapping Rotor Tests





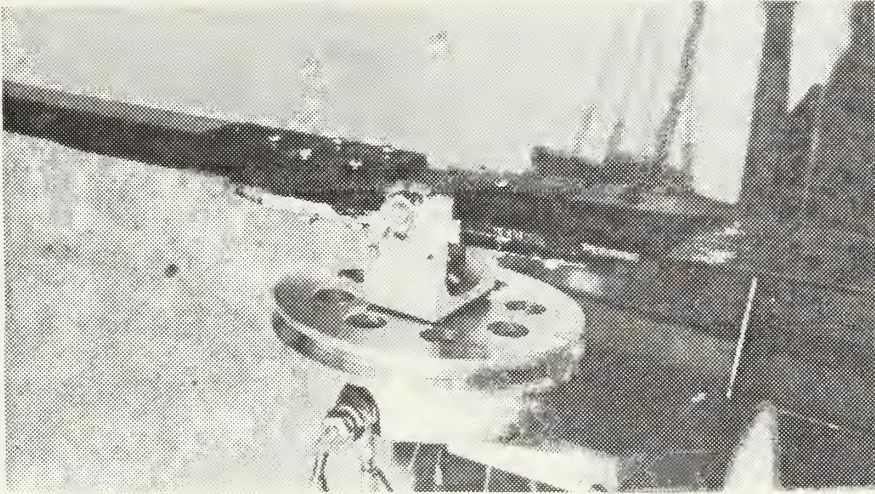


FIGURE IV-2 Rotor Starting Drum

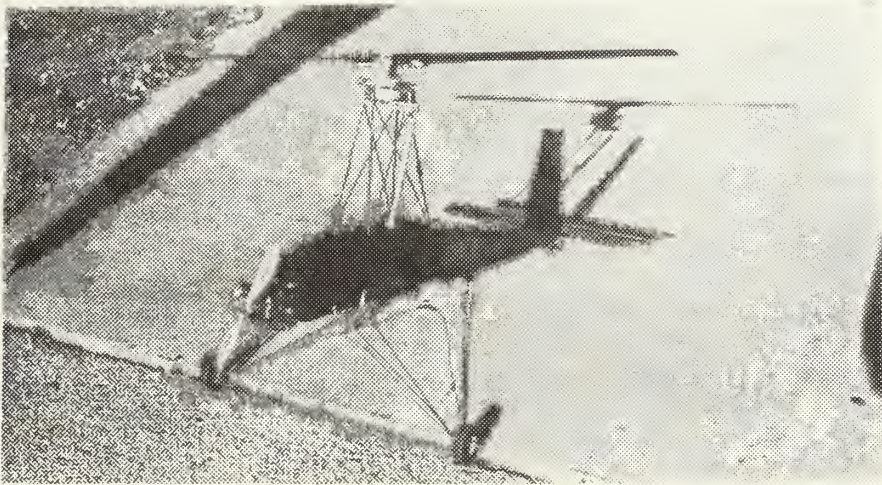


FIGURE IV-3 Two Views of the Final Model Version





The final flight attempt was marginally successful although the model crashed. With the use of the starter drum, the rotor accelerated quite easily during the first part of the take-off run and allowed the model to take off in about a quarter of the distance it had taken previously. The take-off run was directly into the wind.

As the model left the ground, it started a turn to the right (probably due to the head tilt to the right for the purpose of counteracting engine torque). Left head tilt and rudder were applied and the model almost straightened out before the wind and the large pendulum effect (due to the distance the head was above the CG) combined to cause the model to roll even further to the right. As sufficient altitude was not available, the model sideslipped into the ground and shattered the rotor blades. The model did fly, though, and appeared as if it would have handled fairly well. A rotor with augmented flapping stiffness would have provided adequate control power to obviate such control difficulties.

#### B. INITIAL FULL-FEATHERING HEAD TESTS

During the latter stages of model testing, the new rotor head parts were completed, the components assembled and the various linkage connections made. The control rotor was completed by fabricating the control arms out of 1/8-inch piano wire on which the control paddles were mounted, the inner face of each being 5 inches from the control rotor plate. Each paddle had a length of 2 1/2 inches, a chord



of 2 1/8 inches and was constructed similarly to the main blades but additionally incorporated a section of 1/8-inch (inside dimension) square brass tubing. These tubing sections fixed the paddles relative to the tubing (due to the square cross section) and were, in turn, soldered to the control arms thus fixing the paddles on the arms. The two arms were linked together and controlled as shown earlier.

Initially, the head was attached to the upper main rotor shaft (on the rotor test pylon), statically balanced and run with the starter motor. The rotor was positioned horizontally (zero rotor angle of attack), spun up to observe the vibration level and checked to see whether or not the control rotor would follow control commands from the swash plate. The vibration level was excessive, and the control rotor would not follow control inputs.

The blade alignment was checked and found to need further adjustment. This was accomplished and somewhat lessened the vibration, although it was still quite severe. The control rotor was temporarily left as it was. In this state, the pylon and rotor were mounted in the wind tunnel for initial autorotation tests which showed that the rotor would auto-rotate easily enough. The severe vibrations remained, however, and during this initial testing the lateral flexure (on which the strain gages were mounted) was irreparably damaged. The control rotor also continued to resist any attempts to control it.



### C. REDESIGN AND SUBSEQUENT TESTS

In order to get the control rotor working, an attempt was made to give it more power. A new set of control paddles of the same chord but of length  $3 \frac{3}{8}$  inches (as opposed to the  $2 \frac{1}{2}$  inches of the earlier ones) was made and mounted on new arms which increased the distance from the control rotor plate to  $7 \frac{3}{4}$  inches (from the previous 5 inches).

The results showed no improvement; the control rotor would still not follow the inputs from the swash plate. Due to the longer arms, the control rotor was now considerably more flexible, however, and the control arms could be seen to flex in the direction of control input even though the plate would not follow. This suggested that excessive friction somewhere in the system was overpowering the control rotor and keeping it from following.

The source of the friction was narrowed down to the interface of the main-blade brass bearing blocks and the  $\frac{1}{4}$ -inch pivot bolts. Nylon washers were made and inserted into this interface in an attempt to reduce the friction. The results showed that this definitely was the problem area but that the nylon washers were insufficient to solve the problem fully. The severe vibration also remained during these tests.

### D. FURTHER ALTERATIONS AND TESTS

The nylon washers were discarded and replaced by small ball thrust-bearings that were designed for the interface





and virtually eliminated the blade feathering friction. With these bearings in place, the rotor was tested with the result that the control rotor would finally follow the swash plate. The control rotor arm flexibility, which earlier had helped to isolate the problem source, now became a problem itself. Some of the control input was now nullified by this flexing, and the control rotor flapping plane took on the appearance of a saddle.

Even though the system was working at last, the vibration problem remained and the original problem of lift moment dissymmetry was accentuated. Much of the vibration was due to the "linkage slop" that was present due, for the most part, to the reversing links. The main-blade brass bearing blocks also had worn enough to produce a noticeable amount of play.

For the above reasons, the head was disassembled and the bearing blocks bushed to eliminate the play. The head was then assembled with the main-blade control arms linked directly to the swash plate (by-passing the control rotor entirely). This appeared to help somewhat although some vibration remained, possibly due to the fact that the two main-blade feathering axes were not coincident. In order to check this, a simple head junction block was made (FIG. IV-4). With the blades mounted on this block, the resulting vibration was considerably decreased (though not to the level displayed by the free-flapping rotor).



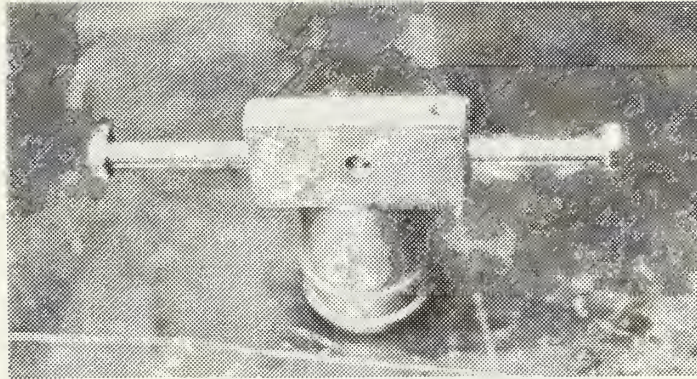


FIGURE IV-4 Head Junction Block

During this latter testing, more substantial flexures were made for the pylon to replace those damaged earlier. In order to isolate the new flexures from much of the vibration (the sinusoidal part of the motion), small hydraulic shock absorbers were made and installed parallel to the lateral and longitudinal force transfer members (FIG. IV-5). These dampers cut down the vibration imposed on the flexures considerably but also added some static friction ("stiction") to the system making good strain gage "zeros" difficult to obtain and maintain.

Despite the above problems, a few runs were made to get a measure of the performance (relative to the free-flapping rotor) of the new head. Approximate values (due to the



uncertain "zeros" caused by the dampers) for the lift, roll moment and drag moment are shown in the table in FIG. IV-6.

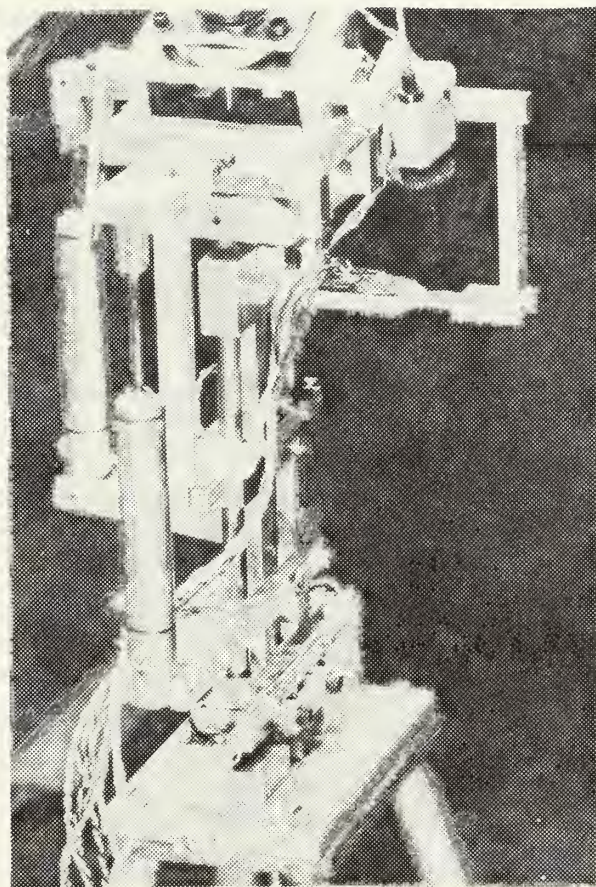


FIGURE IV-5 Hydraulic Vibration Dampers

The roll moments are all to the left, the rotor slowing to a halt when attempts were made to produce roll moments to the right. Runs at higher rotor angles of attack were not attempted due to the extreme vibrations. The disadvantages of this rotor are mainly attributed to the lower rotor speeds





caused, in turn, by the added friction of the swash plate and the greater inertia of the more complex head.

ROTOR ANGLE of ATTACK (DEGREES)	RPM	LIFT (POUNDS)	ROLL MOMENT (INCH- POUNDS)	DRAG MOMENT (INCH- POUNDS)
20	250	1 1/2	1	0
20	440	2 1/3	2	3 1/2
20	450	2 2/3	1	2
20	610	3	4	3
20	630	3	5	4
20	660	3	4	4
25	850	4	3	3

FIGURE IV-6 Table of New Rotor Head Performance Data





## V. DESIGN FEASIBILITY DISCUSSION

The final version of the new rotor head design looks very promising. The full-feathering main rotor system offers a practical solution for the incorporation of augmented flapping stiffness while the free-flapping control rotor provides lateral trim in addition to transmitting cyclic control commands to the main rotor. The final design could be simplified considerably if an alternate method of reversing the control inputs between the free-flapping control rotor and the main rotor were devised. Efforts are continuing along these lines.

No extensive testing of the new head was possible due to the severe vibration levels. What testing was accomplished indicated that the system was performing in the desired manner, however. It was felt that most of the problems encountered, vibration-wise, were due to three reasons.

First, too many adjustments were possible within the system (collective link, swash plate to cyclic input link, all of the reversing arm links, etc.) making system tuning more difficult. A simpler head without, for example, collective control should have been tested and adjusted initially. Then, when the collective control was added, new problem areas could have been more easily traced.

Second, the number of linkages in the system eventually created an excessive amount of play. Play in the system is nearly synonymous with vibration about which little can be



done. Some of this play was due to the use of relatively soft bushing-type bearings (brass). These not only wore fairly quickly (in the case of the main blade bearing blocks) but also produced sufficient friction to hamper the control mechanism. Suitable bearings (like small ball bearings) should have been used, especially for the high-load sections (such as the main blade feathering bearings).

Third, as was discussed earlier in the testing section, the fact that the feathering axes of the two main blades were not coincident caused an additional input to the vibration level. If these problems had been avoided, it is felt that the vibration level would have approached that of the free-flapping rotor initially tested.

Due to the fact that the free-flapping rotor was tested with the same main blades as the full-feathering head, the use of inflexible blades was not considered to add appreciably to the vibration level of the new head. The inflexible blades, therefore, remain feasible, at least for small rotors. Finally, as no comparison was made with a similar set of flexible blades, the effect of blade flexibility was not included per se in this study.



## VI. CONCLUSIONS

The new rotor control scheme (the free-flapping control rotor) appears to be feasible as a practical design. Besides conveying cyclic control commands to the main rotor, it also provides lateral trim with varying forward speed. The free-flapping control rotor, therefore, offers a simple, mechanical means of main rotor control, especially for systems employing augmented flapping stiffness.

Augmented flapping stiffness is being incorporated in modern rotorcraft not only because it gives enhanced control power but because control is substantially independent of rotor thrust. Considering this, the use of lateral trim by cyclic main blade feathering seems to offer a most efficient and flexible approach.

With full control over main blade feathering, relatively inflexible rotor blades seem feasible if vibration isolation means are used to minimize the level of vibration transferred to the fuselage. Also, the inflexible blades would appear to be appropriate for smaller rotors with higher disk loadings.

The use of radio-controlled freely-flying models definitely has a place in experimental work. The flying, though, should be done in the final stages after at least preliminary testing has been accomplished in a wind tunnel. The flying model gives a good indication of the stability and handling



characteristics, but due to the small size, is quite sensitive to wind and turbulence, especially during the critical phases of flight (mainly take-off and landing). The small size also makes observation of the exact sequence of events following a disturbance difficult when the model is in flight. If these limitations are taken into consideration, the use of flying models is strongly recommended for testing purposes.





## APPENDIX A. LIFT MOMENT DISSYMMETRY

The source of the lateral lift moment dissymmetry is the horizontal translation of a rotating, lifting rotor. This can be shown by examining the velocity profile along the blades resulting from rotary motion alone, translatory motion alone, and finally the combined motion. (FIG. A1). Examining the velocity distribution is sufficient as the lift (and hence the lift moment) is a function of the square of the velocity.

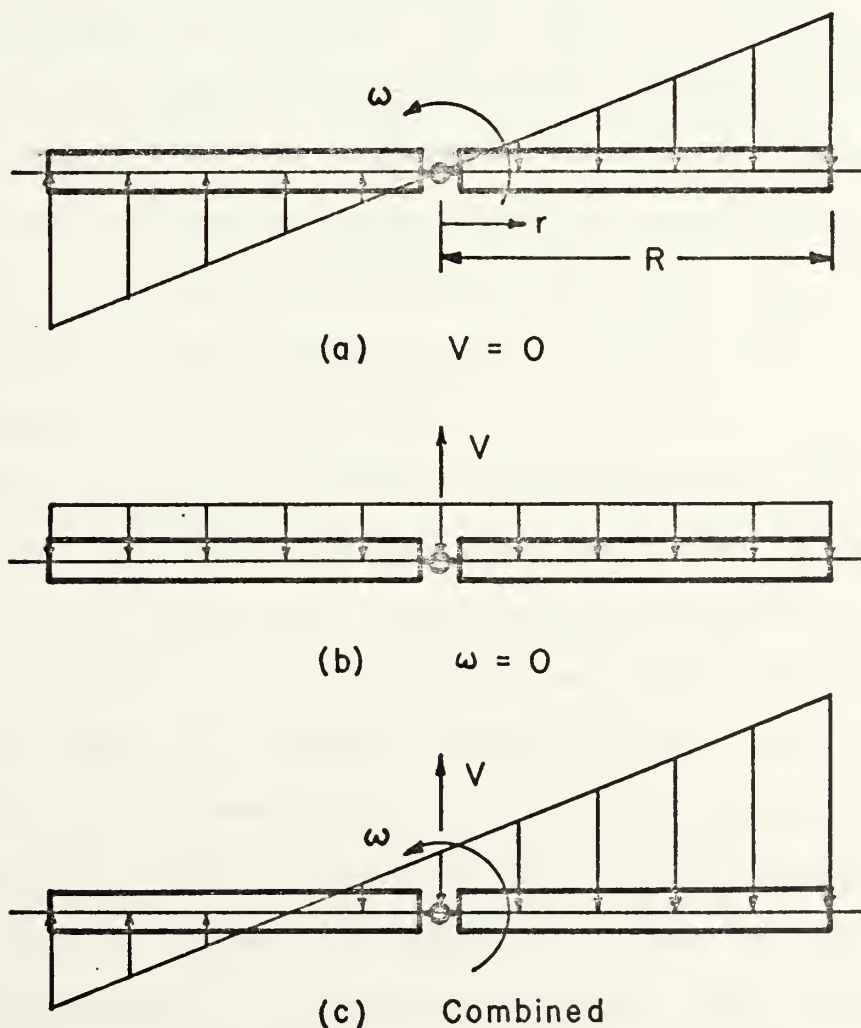


FIGURE A1 Blade Velocity Distribution



FIGURE A1 shows the rotor in planform as seen from above with the blades in the  $\psi = 90^\circ$  and  $\psi = 270^\circ$  positions, the  $\psi = 0^\circ$  reference being the downstream position and rotation being in the counter-clockwise sense.

In (a), the translational velocity,  $V$ , is zero (corresponding to a tip-speed ratio,  $\mu$ , of 0) and the local velocities are produced wholly by rotation, i.e.,  $\omega r$  where  $r$  is the spanwise station of interest and  $R$  is the blade radius. The roles are reversed in (b) with the rotational velocity,  $\omega$ , equal to zero (corresponding to a  $\mu$  of  $\infty$ ) and the local velocities equal to  $V \sin \psi$ . Note that in (b) reverse flow (flow from the trailing edge to the leading edge of the blade) exists on the retreating ( $\psi = 270^\circ$ ) blade. The combined or total resultant velocity distribution is shown in (c) and is equal to the addition of those in (a) and (b), i.e.,  $\omega r + V \sin \psi$ . Two important factors can be noted from this distribution.

Firstly, the average velocity over the retreating blade is less than that over the advancing blade due, in part, to the area of reversed flow. This velocity difference produces, as stated earlier, a difference in the lift of the two blades which is a direct function of the tip-speed ratio and hence, for a given rotor operating at a constant  $\omega$ , of the forward velocity. Restating this, the difference in the lift of the two blades, and therefore in the lift moment, is a direct function of the forward velocity. This, basically, is the lift moment dissymmetry problem.



Secondly, the region of reversed flow over the retreating blade gives it an entirely different velocity (and lift) distribution from that of the advancing blade. This distribution difference causes varying spanwise blade loading as the blade proceeds around the circle which, in turn, produces vibrations in the system at a two-per-revolution frequency. This vibration is inherent in a two-bladed system even though the lift of the two blades is controlled to produce a zero net moment at the hub. This is best shown with an example.

#### EXAMPLE

For this example, the translational and rotational velocities and the resultant tip-speed ratio will be as follows:

$$V = 100 \text{ ft/sec}$$

$$\omega = 300/R \text{ rad/sec}$$

$$\mu = 1/3$$

The local blade section velocity,  $v$ , is given by

$$v = \omega r + V \sin \psi$$

and the velocity profile is shown in FIG. A2.

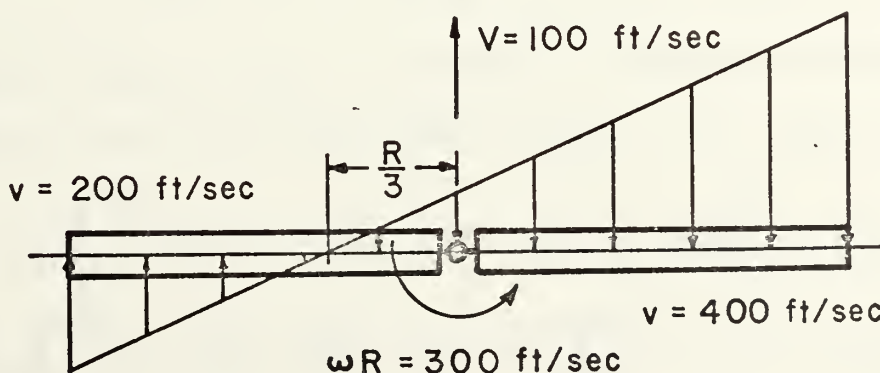


FIGURE A2 Example Velocity Distribution



The lift on a blade element is given by

$$dL = \frac{1}{2} \rho v^2 C_l C dr$$

where, for a constant-chord blade, the area,  $S$ , is

$$S = \int_0^R C dr = C \int_0^R dr$$

which finally gives the lift as

$$L = \frac{1}{2} \rho C C_l \int_0^R [v(r)]^2 dr$$

This involves an approximation which assumes a constant lift coefficient along the blade.

The moment at the rotor hub is just the first moment of the lift around the blade root.

$$M_H = \int_0^R r dL = \frac{1}{2} \rho C C_l \int_0^R r [v(r)]^2 dr$$

The moments, therefore, on the advancing and retreating blades are, respectively

$$M_{HA} = \frac{1}{2} \rho C C_{lA} \int_0^R r (100 + 300 \frac{r}{R})^2 dr$$

$$M_{HR} = \frac{1}{2} \rho C C_{lR} \int_0^R r (-100 + 300 \frac{r}{R})^2 dr$$

In order to have a zero net moment at the hub, the moments produced by the two blades must balance, i.e.,  $M_{HR} = M_{HA}$ .

$$\frac{1}{2} \rho C C_{lA} \int_0^R r (100 + 300 \frac{r}{R})^2 dr = \frac{1}{2} \rho C C_{lR} \int_0^R r (-100 + 300 \frac{r}{R})^2 dr$$

$$C_{lA} \int_0^R r (1 + 6 \frac{r}{R} + 9 \frac{r^2}{R^2}) dr = C_{lR} \int_0^R r (1 - 6 \frac{r}{R} + 9 \frac{r^2}{R^2}) dr$$

$$\frac{19}{4} C_{lA} = \frac{3}{4} C_{lR}$$





This shows that, when the rotor is perpendicular to the flow, the lift coefficient of the retreating blade must be 6.33 times that of the advancing blade in order to balance the lateral moments. (When the blade is parallel to the flow, this lift coefficient difference reduces to zero.)

The above analysis is somewhat in error in that the area of reversed flow would produce negative lift or would be stalled giving virtually no lift instead of that obtained by the strict utilization of the velocity profile. Modifying the lift and moment equations for the retreating blade to take this into account yields the following equations.

$$\begin{aligned}
 L_R &= \frac{1}{2} \rho C \left( 0 \cdot \int_0^R [v(r)]^2 dr + C_{1R} \int_0^R [v(r)]^2 dr \right) \\
 &= \frac{1}{2} \rho C C_{1R} \int_0^R \left( -100 + 300 \frac{r}{R} \right)^2 dr \\
 M_{HR} &= \frac{1}{2} \rho C C_{1R} \int_0^R r \left( -100 + 300 \frac{r}{R} \right)^2 dr \\
 &= \frac{1}{2} \rho C C_{1R} (10^4) (R^2) \left( \frac{20}{27} \right)
 \end{aligned}$$

When this is substituted for the earlier value to balance  $M_{HA}$ , the retreating blade lift coefficient,  $C_{1R}$ , is seen to equal  $6.41 C_{1A}$  vice the  $6.33 C_{1A}$  obtained earlier.

#### END EXAMPLE

The attempt to vary the average lift and lift distribution along the blade sets up a two-per-rev vibration. The use of relatively inflexible blades has the tendency of assuring that these vibrations get passed on to the rotor hub. In order



not to pass these vibrations on to the fuselage, a means of isolation must be formed between the main rotor shaft and the fuselage.



## APPENDIX B. WIND TUNNEL AND AIRSPEED MEASUREMENT SYSTEM

The wind tunnel testing phase of this investigation was performed in the RINGLEB-type smoke tunnel at the Naval Postgraduate School (FIG. B1). Although the smoke visualization feature was not used, the tunnel offered the largest test section at the school and had a sufficient velocity range for the desired testing.

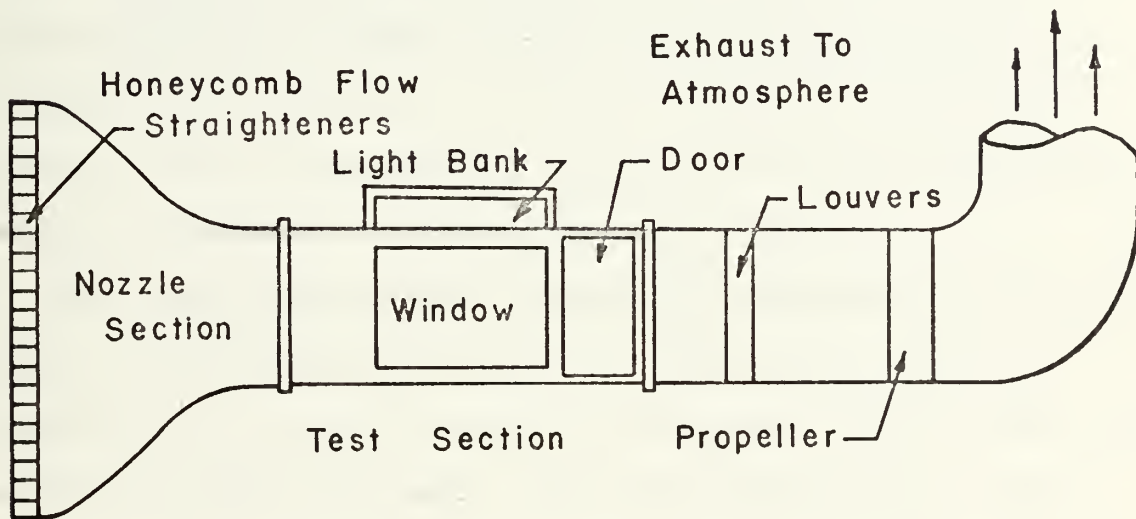


FIGURE B1 Naval Postgraduate School Smoke Tunnel

The tunnel has an initial inlet section with dimensions of 15 by 15 feet which is then reduced to a test section of 5 by 5 feet. The air is drawn into the tunnel through the inlet section which consists of pieces of approximately four-inch thick aluminum honeycomb acting as flow straighteners. A converging nozzle is used next to neck down the flow to the



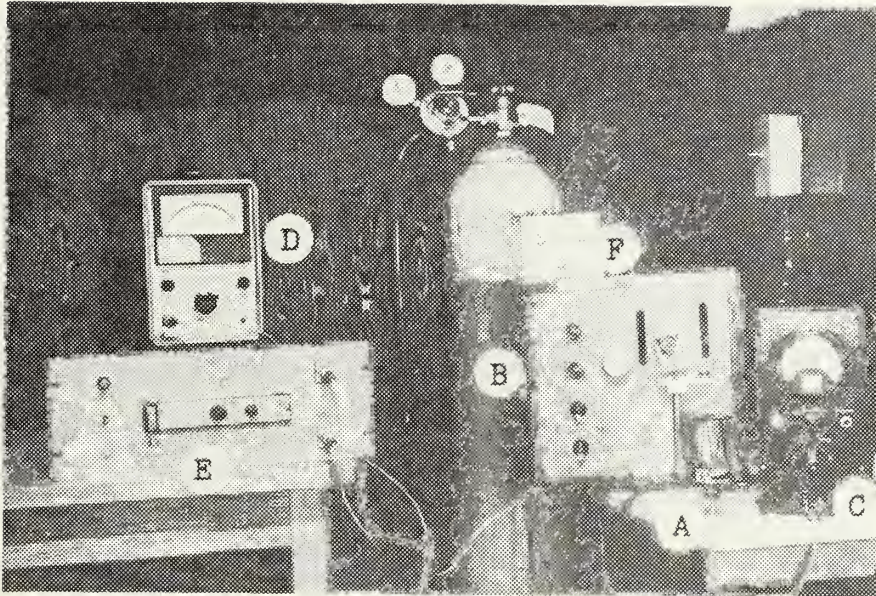


size of the test section. The air then proceeds through the test section and a set of louvers which help prevent disturbances from the propeller section moving back upstream to the test section during slow speed operation. After the air has been drawn through the propeller section, it is exhausted away from the tunnel.

The air velocity capability of the tunnel was in the range of 0-32 feet per second (0-22 MPH) as measured with a U-tube manometer connected to a static port in the wall of the test section. This system, although possessing good accuracy, was difficult to use and displayed a definite settling time. Therefore, a system was desired that would be both reasonably accurate and easy to use.

The head element from a hand-held anemometer of the type used by meteorologists (Detector, T-321C/PMQ-3; Part No. 58A42D1-44), actually a small AC generator, was obtained and mounted in the tunnel wall. The leads were run to an AC voltmeter (Ballantine Laboratories Model 643) through a trimming potentiometer which allowed the maximum tunnel velocity to be set equal to the full-scale meter deflection. The system was calibrated against the manometer and resulted in an easily used airspeed system of sufficient accuracy for this work. The calibrating manometer, anemometer head element and AC voltmeter are shown in FIG. B2.





- A - Anemometer Head Unit
- E - U-Tube Anemometer Instrument
- C - AC Voltmeter, Airspeed Readout
- D - Micro Voltmeter, Strain Gage Readout
- E - Strain Gage Signal Amplifier
- F - Strain Gage Trim System

FIGURE B2 Smoke Tunnel Test Equipment



## APPENDIX C. ROTOR TEST PYLON

During the construction stages of the new rotor head, it became apparent that suitable testing facilities were not available. In order to utilize the smoke tunnel, a means of mounting the head had to be devised. Therefore, the design of a rotor test pylon was initiated. To ensure the lasting value of the pylon, the design was to incorporate a sufficient number of features for it to be usable for similar future projects.

The design requirements were that the pylon be able to measure lift (vertical forces), lateral (rolling) moments and a combination of longitudinal (pitching) and drag-produced moments. The three measurements were to be independent and capable of being read, if not simultaneously, relatively quickly. To facilitate the investigation of the various rotor working states and autorotation, the upper section of the pylon had to be able to tilt, longitudinally, through roughly  $\pm 30^\circ$ . Finally, a means had to be provided to power the rotor, or at least start it in the case of autorotation, from outside the tunnel.

The pylon initially was designed around a mechanical balance system, but recommendations by one of the technicians subsequently changed this to a strain-gage balance system. Each flexure was instrumented with four gages (two above and two below) to form a full bridge arrangement which was,





therefore, temperature compensating. The strain gage signals were routed through a switching system, amplified and displayed on a voltmeter (Hewlett Packard Model 425A Micro Volt-Ammeter). The switching system allowed display of the reading from any one of the three sets of gages on the meter. Calibration of the three systems (by adjustment of the three individual power supplies and amplifier gains) allowed the readings to be adjusted to read out in desired engineering units (pounds of lift, inch-pounds of lateral moment, etc.) while a trim system allowed each function to be zeroed for each series of tests. Two views of the basic pylon and the basic strain gage layout are shown in FIGS. C1 and C2 respectively.

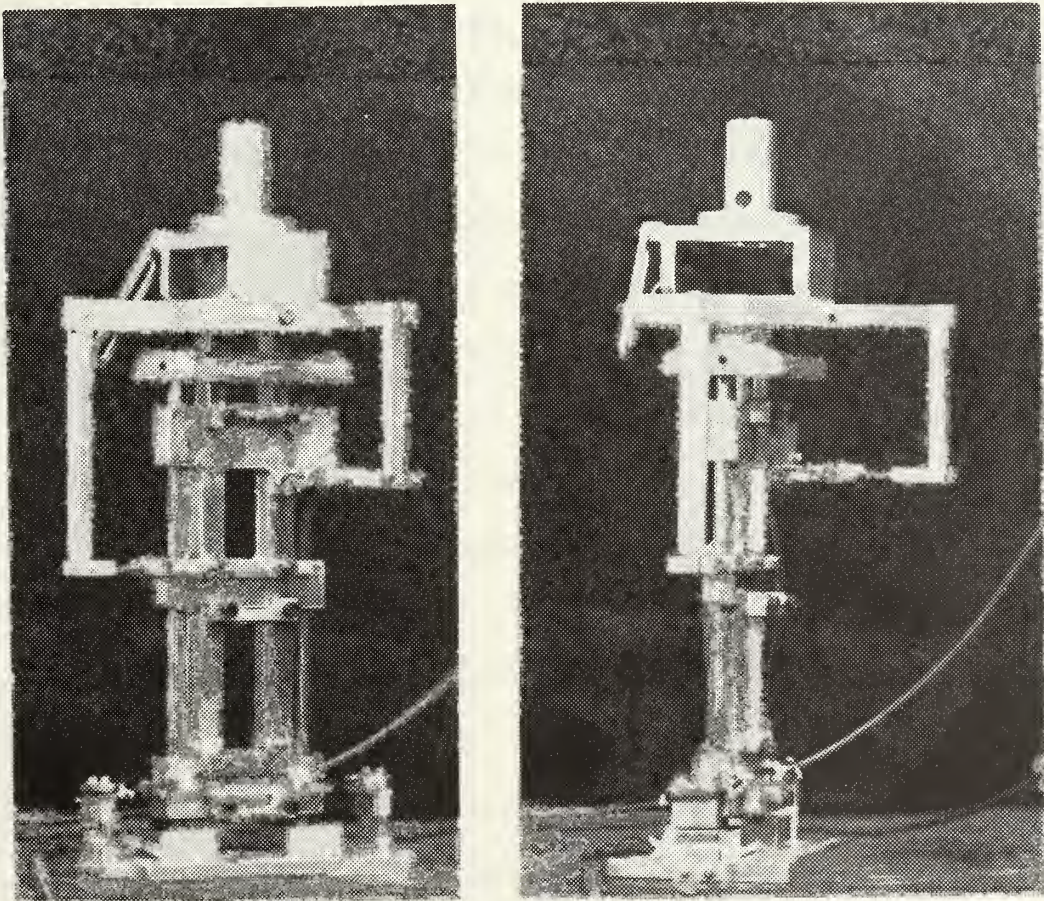


FIGURE C1 Two Views of the Rotor Test Pylon





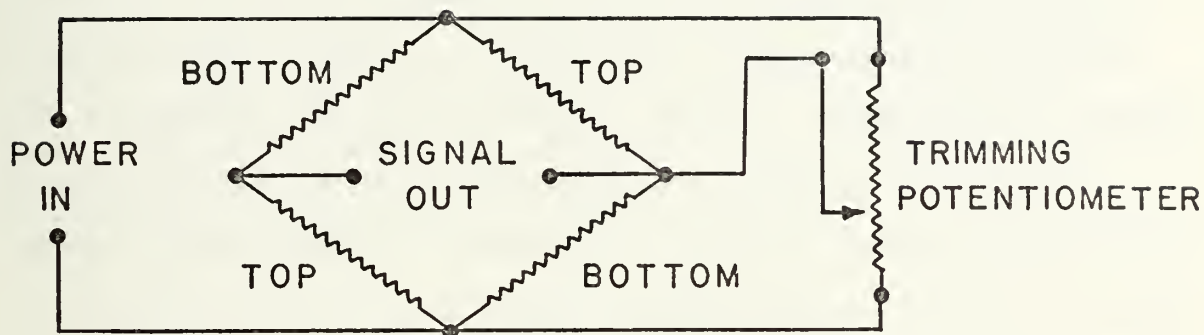


FIGURE C2 Strain Gage Bridge and Trim System

An interface between the test pylon and the head was designed and built in the form of a conventional swash plate. This was basically a two-row, ball-race bearing with the inner race linked to the pylon through a two-degrees-of-freedom gimbal system and the outer race (driven by the rotor shaft to maintain synchronization with the rotor head) linked to the cyclic control input arm for the transmission of control commands. The swash plate was controlled by two small servo motors which were controlled, in turn, from outside the test section thus allowing the cyclic pitch control to be exercised during tunnel runs. The collective pitch was fixed for any given run, however, and could be changed only by stopping the tunnel and changing it at the head.

Finally, a model aircraft starter motor was added to the lower part of the pylon. This was set up so that it could be engaged and run from the tunnel control station. The



motor had a rubber cup on the drive end which could be brought to bear on an aluminum disk attached to the lower end of the main rotor drive shaft. A universal joint was inserted in the main rotor shaft to allow the starter to turn the lower section of the shaft while allowing the upper shaft section, with the upper section of the pylon, to be tilted fore and aft to change the rotor angle of attack. Engaging the starter motor invalidated the lift readings, though, so the motor eventually was used to initiate autorotation only. Two views of the final rotor test pylon with the new rotor head in place are shown in FIG. C3, one view with the starter engaged and the other with it disengaged.

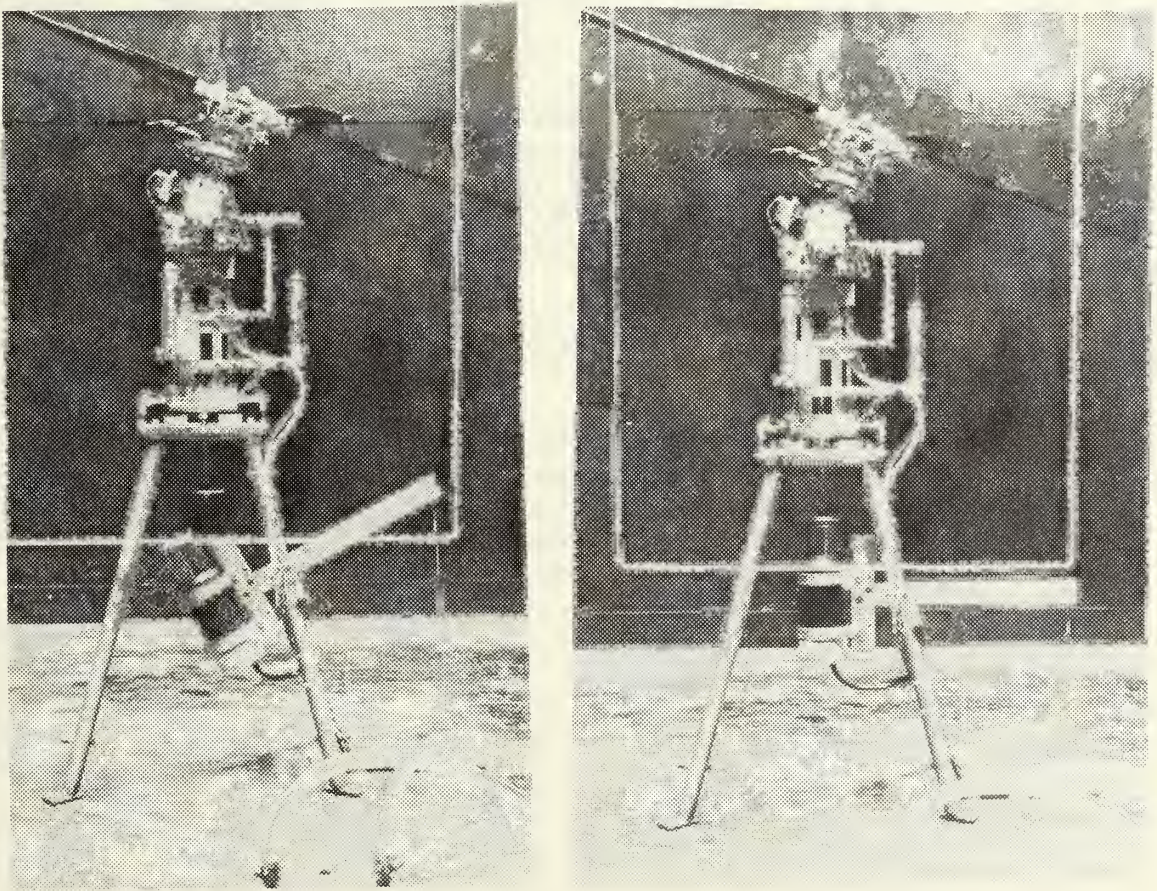


FIGURE C3 Test Pylon with Full-Feathering Head





## APPENDIX D. FINAL HEAD DRAWINGS AND PHOTOGRAPHS

In this section are contained the detail drawings for the main parts made for the two rotor systems, drawings of the full-feathering head assembly and photographs of the head mounted on the rotor test pylon. An index to the drawings and photographs is given below.

### DRAWINGS

#### 1. Free-Flapping Rotor

Figure D1	Rotor Base Plate
Figure D2	Base Plate Pivot Block

#### 2. Full-Feathering Rotor

Figure D3	Reversing Link Base Plate
Figure D4	Main Rotor Head Core Element
Figure D5	Control Rotor Base Plate
Figure D6	Main Blade Attachment Unit
Figure D7	Assembled Rotor Head

### PHOTOGRAPHS

Figure D8	Two Views of Mounted Rotor Head
Figure D9	Two Views of Mounted Rotor Head
Figure D10	Two Views of Mounted Rotor Head
Figure D11	Two Views of Mounted Rotor Head
Figure D12	Two Views of Rotor Test Set-Up

All drawings are full scale.



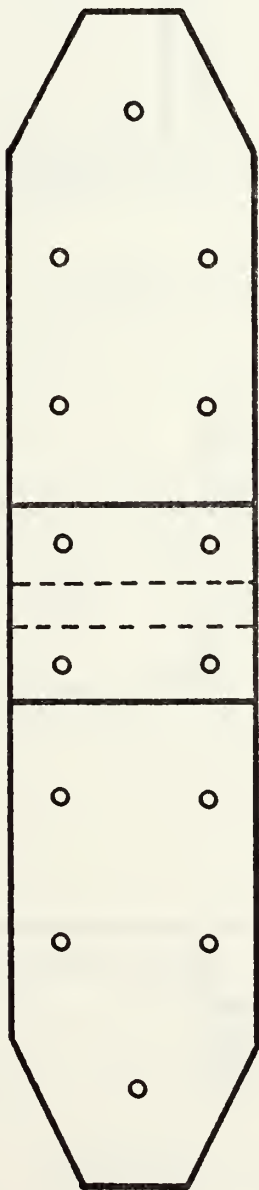
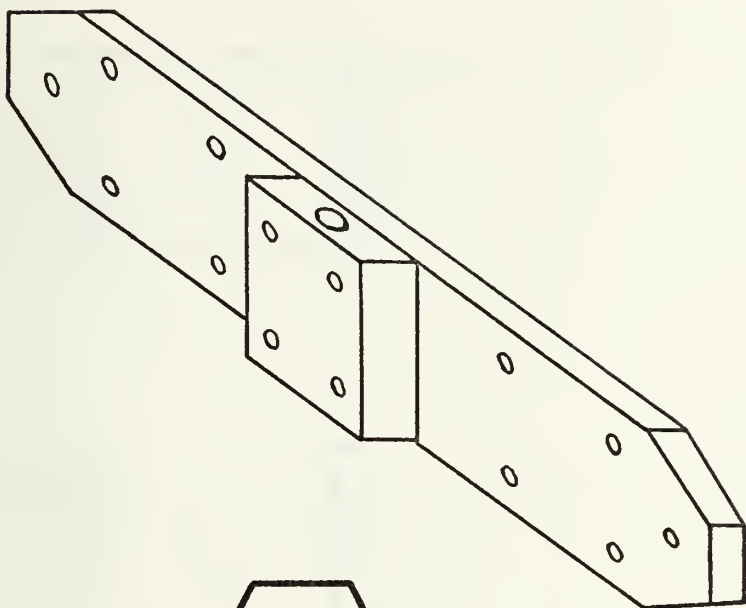


FIGURE D1 Rotor Base Plate





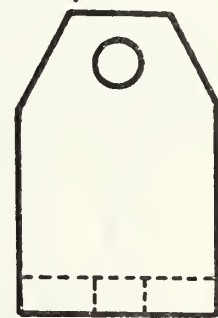
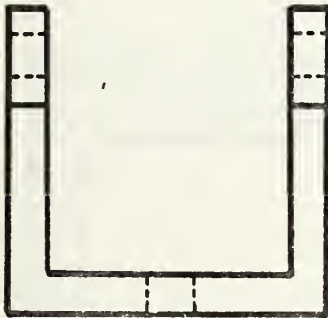
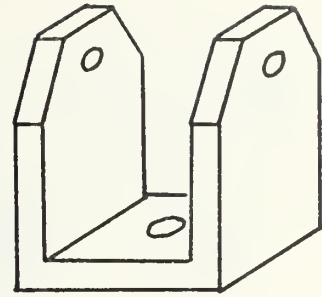
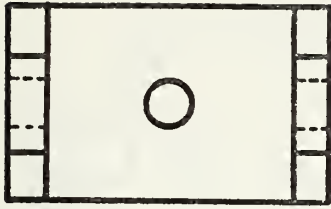


FIGURE D2 Base Plate Pivot Block

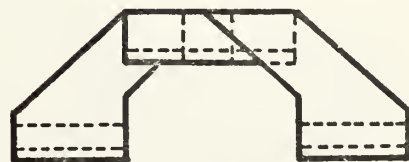
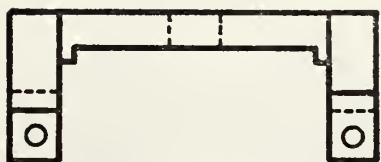
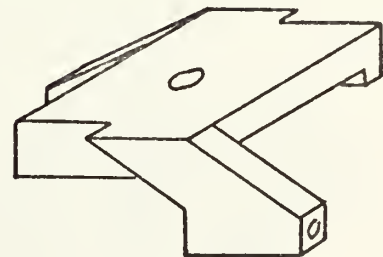
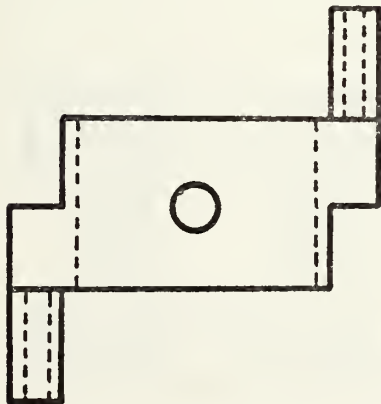


FIGURE D3 Reversing Link Base Plate



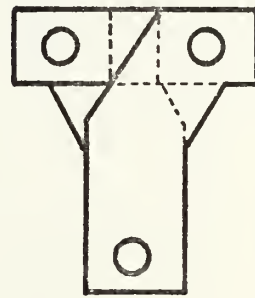
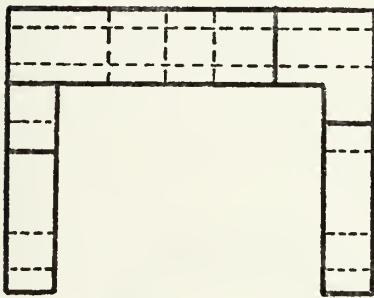
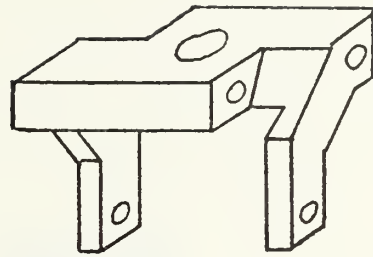
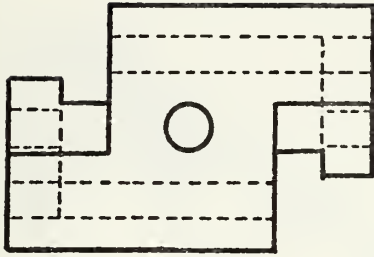


FIGURE D4 Main Rotor Head Core Element

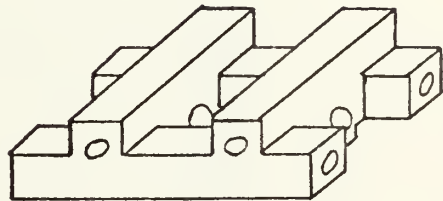
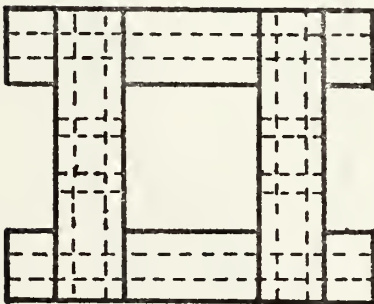


FIGURE D5 Control Rotor Base Plate



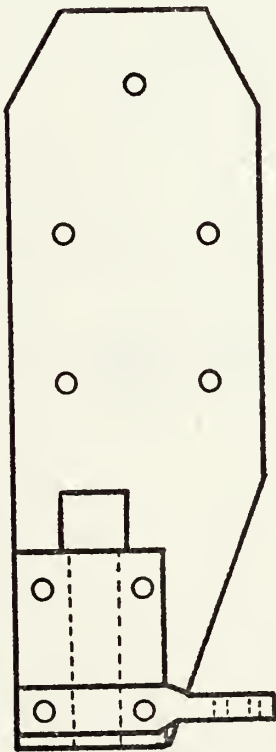
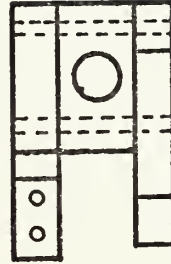
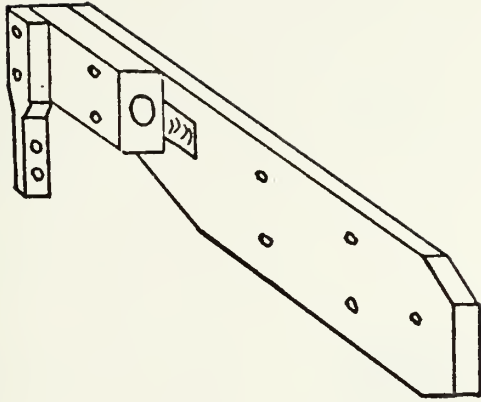
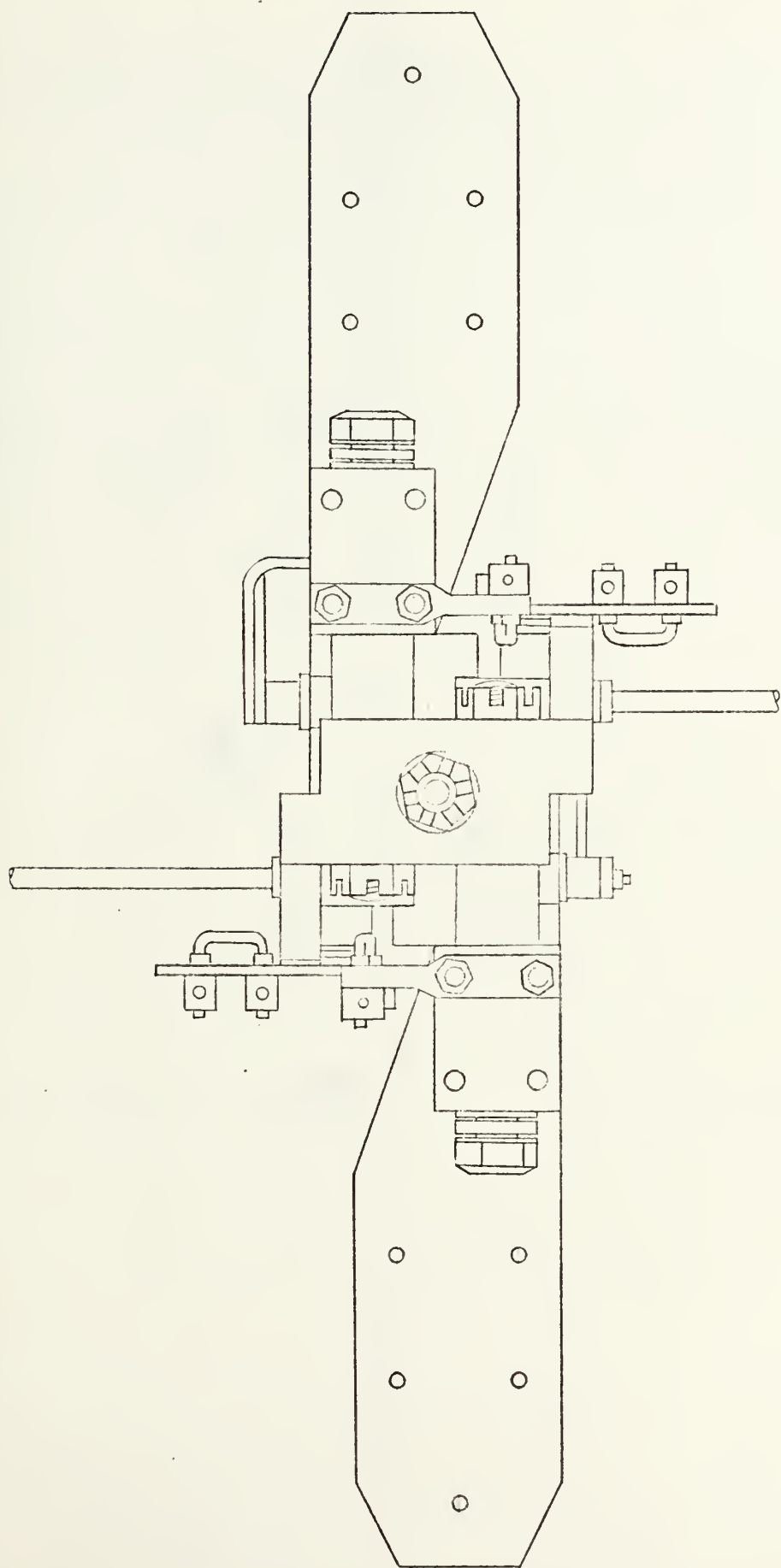


FIGURE D6 Main Blade Attachment Unit



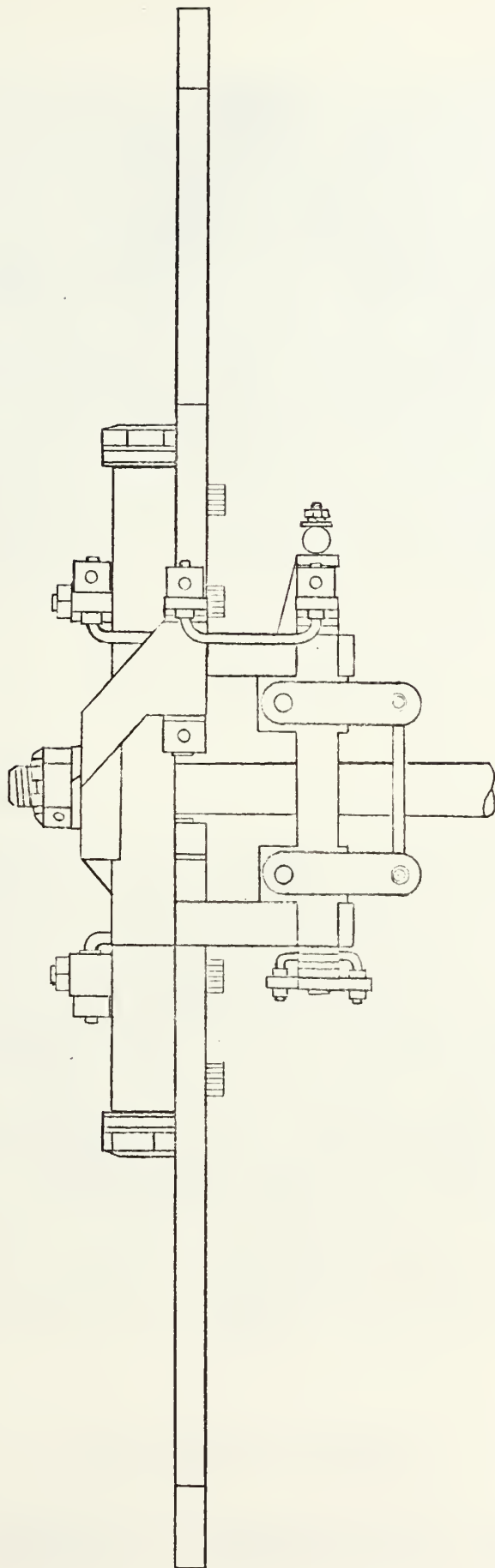


(a) Top View

FIGURE D7 Assembled Rotor Head



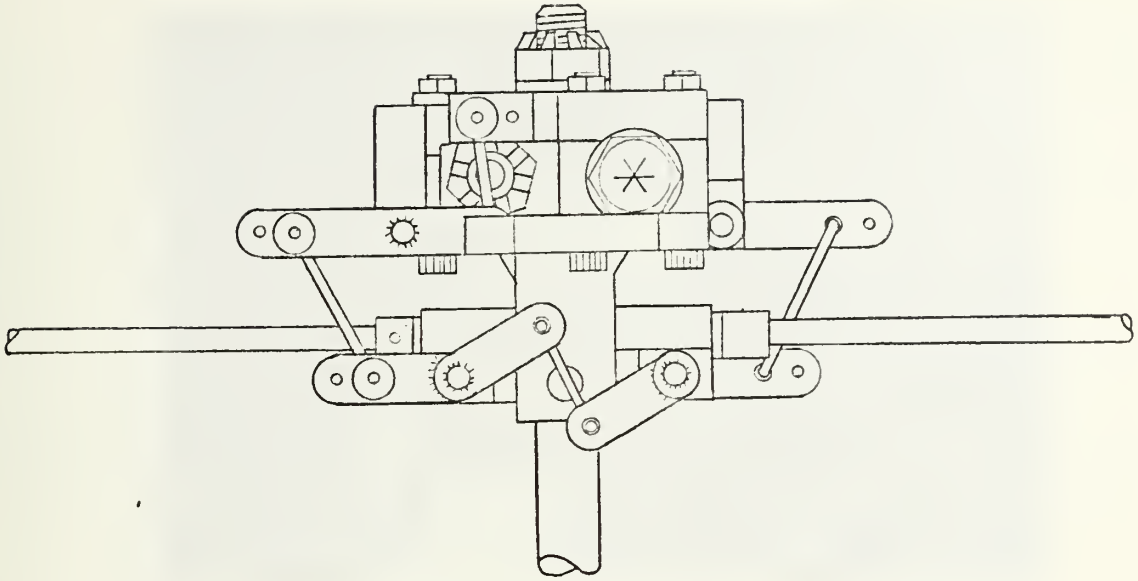




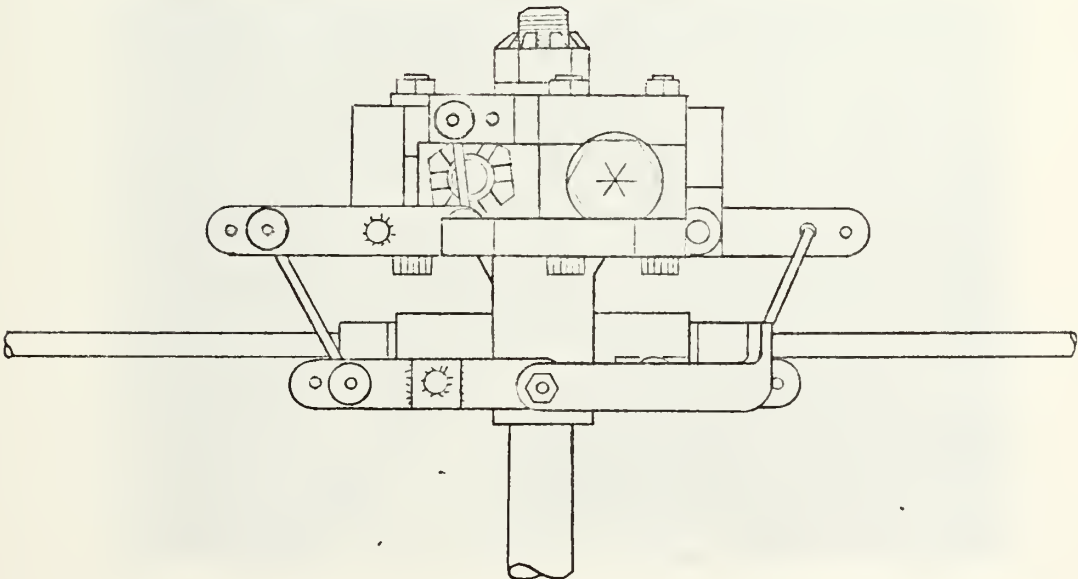
(b) Front View

FIGURE D7 Assembled Rotor Head





(c) Left End View



(d) Right End View

FIGURE D7 Assembled Rotor Head



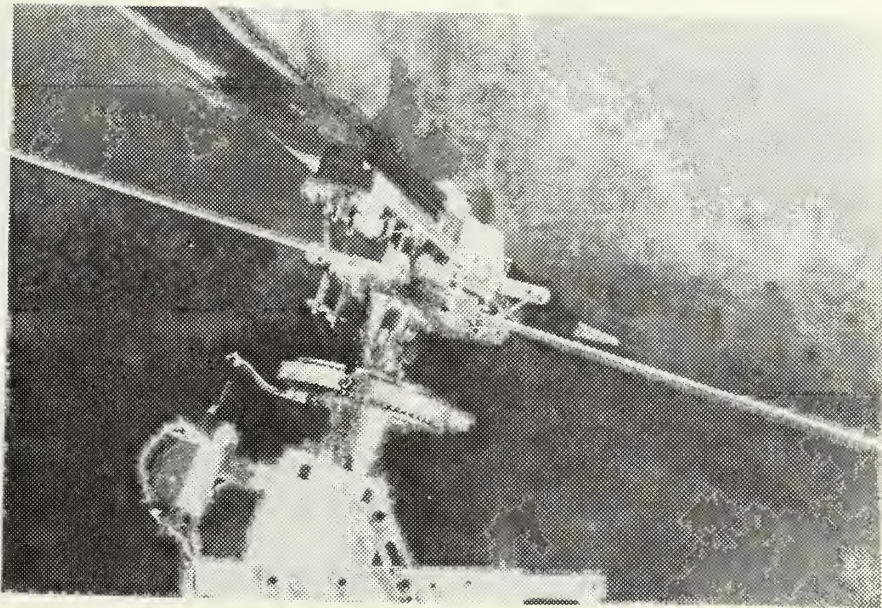
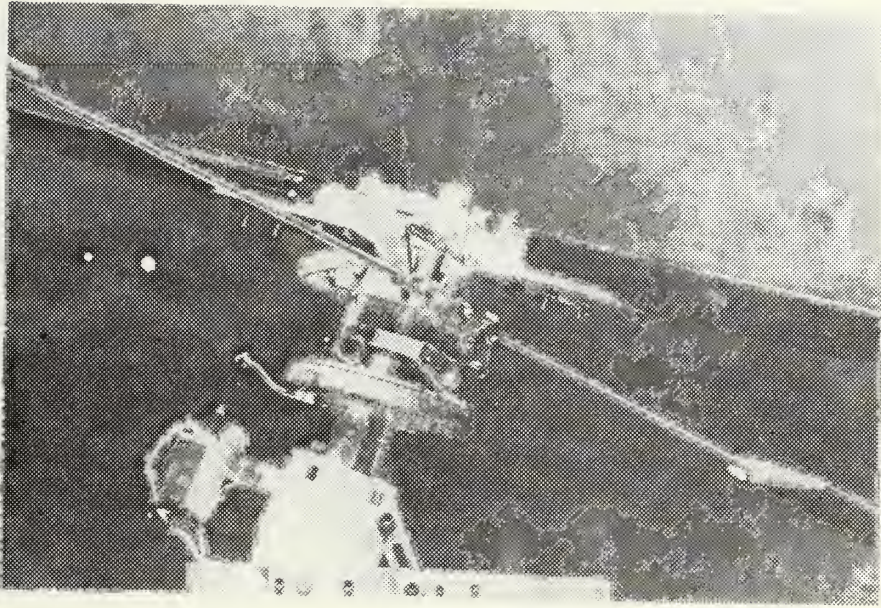


FIGURE D8 Two Views of Mounted Rotor Lead





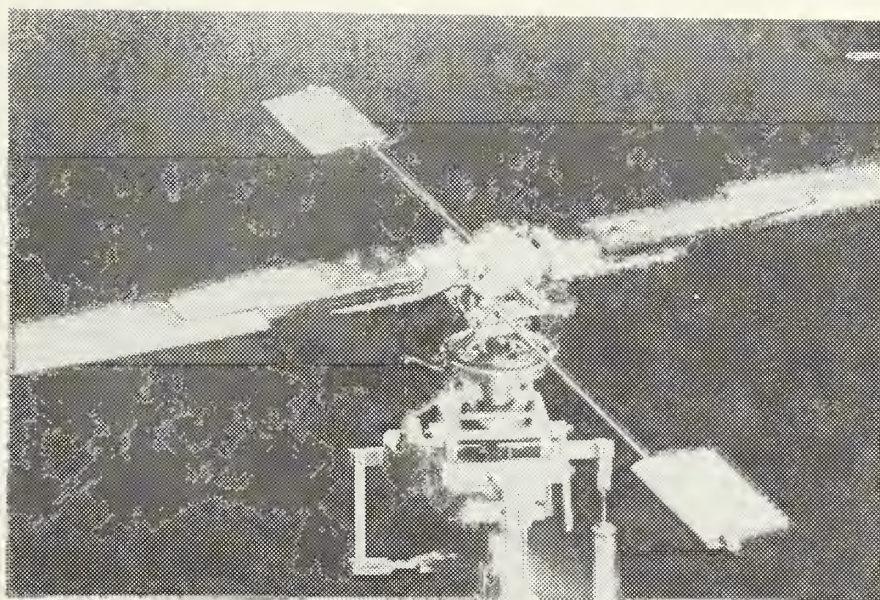
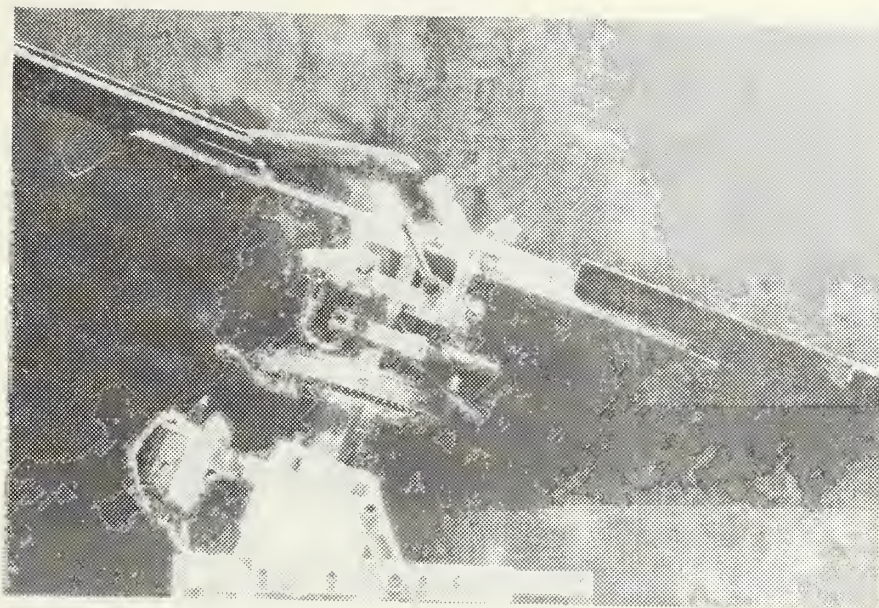


FIGURE D9 Two Views of Mounted Rotor Head





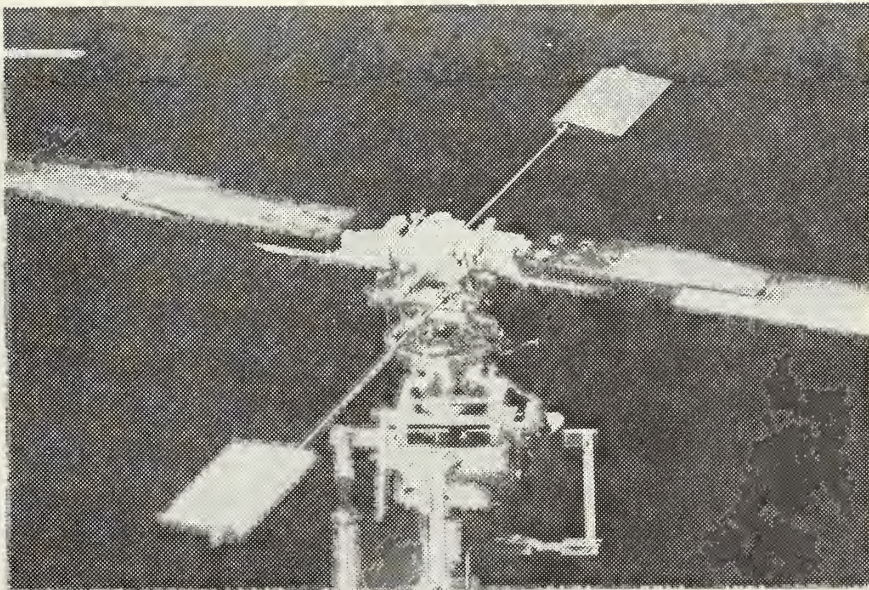
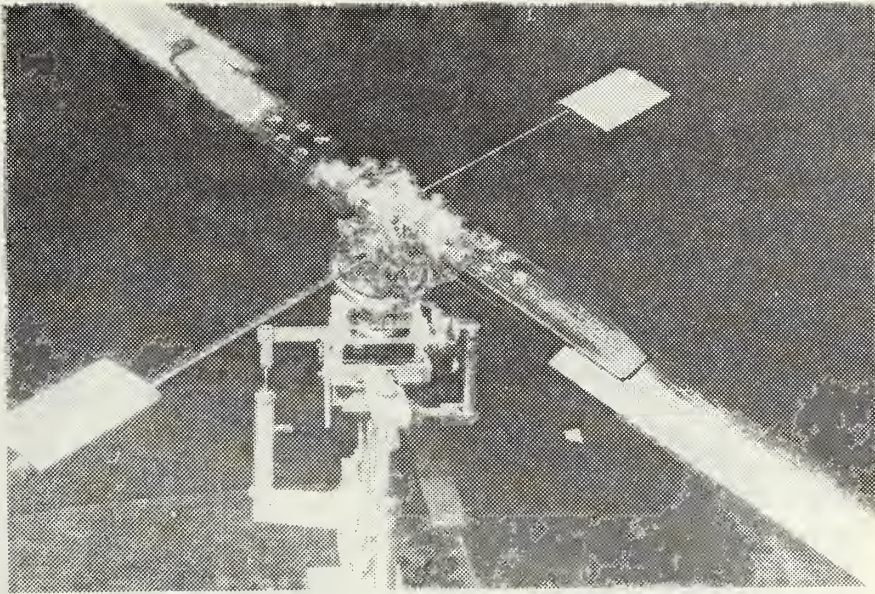


FIGURE D10 Two Views of Mounted Rotor Head





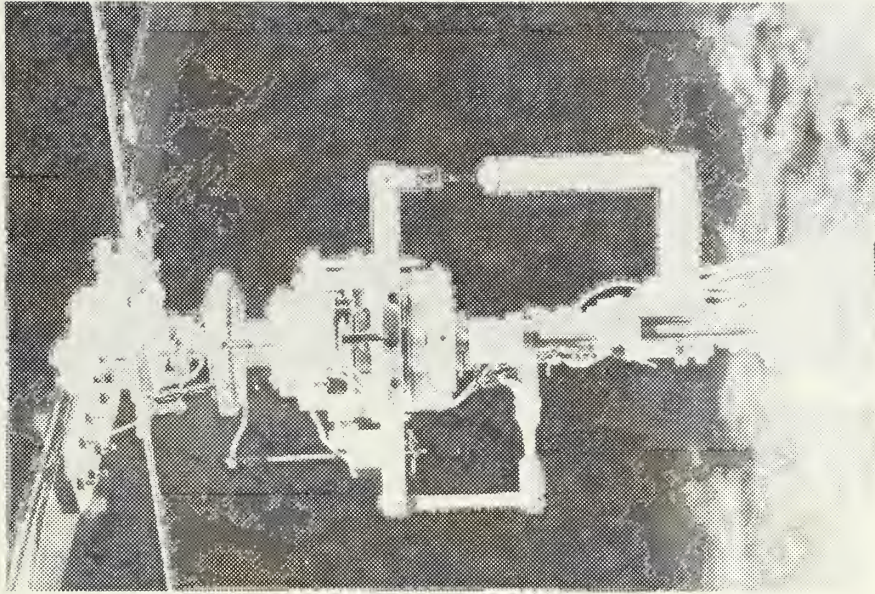
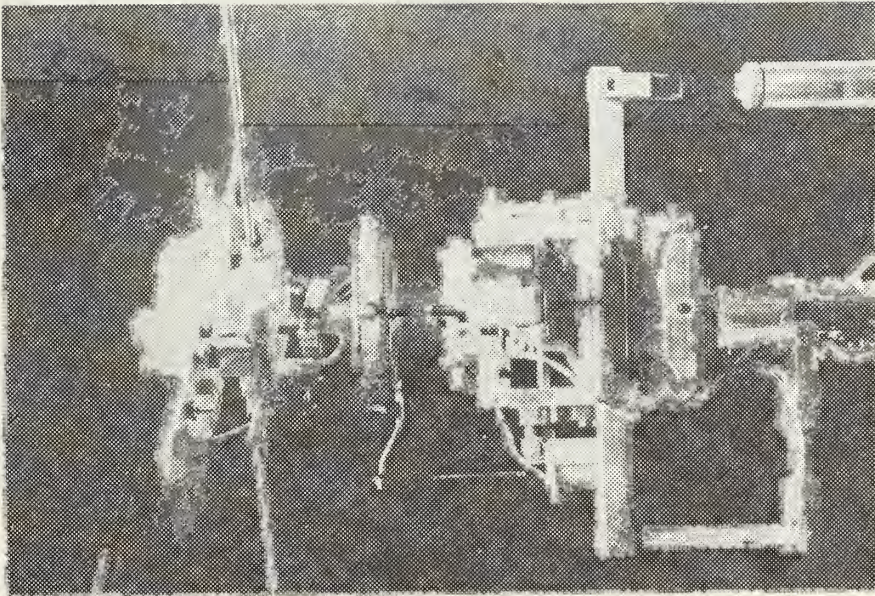
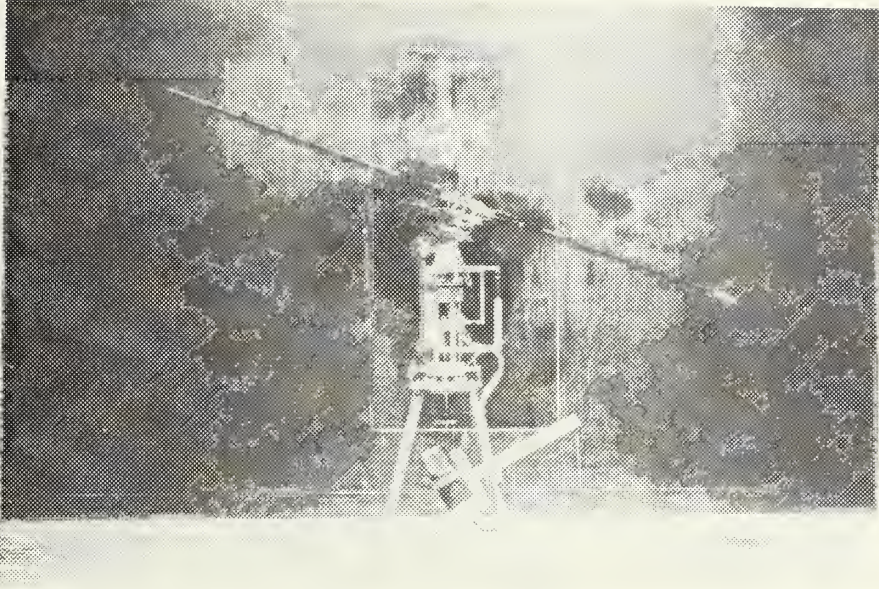


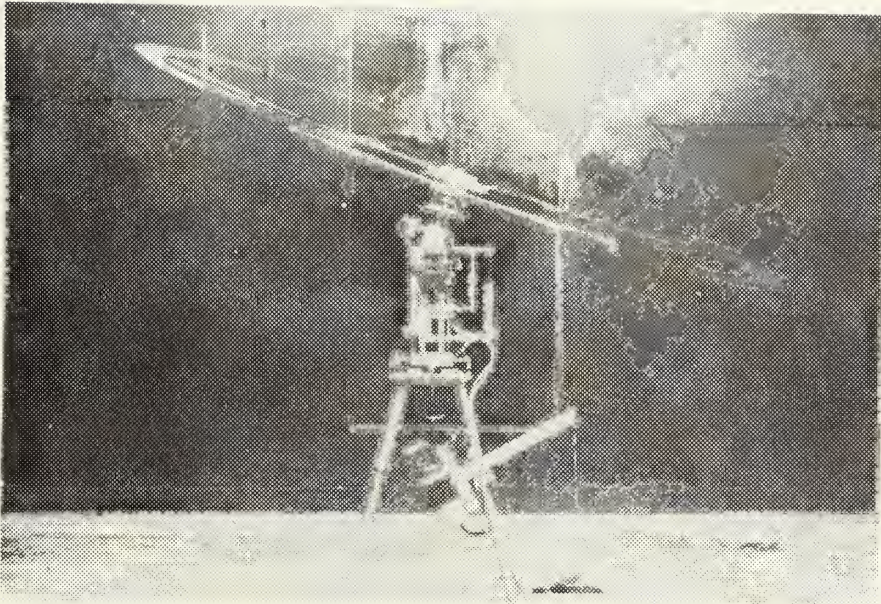
FIGURE D11 Two Views of Mounted Rotor Load







(a) Rotor Stationary



(b) Rotor in Operation

FIGURE D12 Two Views of Rotor Test Set-Up



## BIBLIOGRAPHY

1. Bennett, J. A. J., "The Era of the Autogiro," The Journal of the Royal Aeronautical Society, Vol. 65, No. 610, p. 649-660, October 1961.
2. Gessow, A. and Meyers, G. C., Aerodynamics of the Helicopter, Frederick Unger Publishing Company, New York, 1952.
3. Naval Air Engineering Laboratory Report NAEL-ENG-6818, The Three Dimensional Smoke Tunnel of the Naval Air Engineering Laboratory in Philadelphia, Pennsylvania, by Friedrich O. Ringleb, 10 July 1961.
4. Payne, P. R., Helicopter Dynamics and Aerodynamics, Sir Isaac Pitman & Sons, Ltd., 1959.
5. Simons, I. A., "Some Objectives and Problems Associated with Model Testing," The Aeronautical Journal of the Royal Aeronautical Society, Vol. 74, p. 539-548, July 1970.
6. Stuart, J., III, "The Helicopter Control Rotor," Aeronautical Engineering Review, Vol. 7, No. 8, p. 33-37, August 1948.





# INITIAL DISTRIBUTION LIST

	No. Copies
1. Defense Documentation Center Cameron Station Alexandria, Virginia 22314	2
2. Library, Code 0212 Naval Postgraduate School Monterey, California 93940	2
3. Chairman, Department of Aeronautics Naval Postgraduate School Monterey, California 93940	1
4. Professor J.A.J. Bennett, Code Zn Department of Aeronautics Naval Postgraduate School Monterey, California 93940	1
5. Lt. Richard A. Wiley, USN HS-15 NAS Lakehurst New Jersey 08733	1
6. Lt. William A. Simmons, USN 413 North Main Street Stockton, Illinois 61085	1



UNCLASSIFIED

Security Classification

## DOCUMENT CONTROL DATA - R &amp; D

(Security classification of title, body of abstract and indexing annotation must be entered when the overall report is classified)

1. ORIGINATING ACTIVITY (Corporate author) Naval Postgraduate School Monterey, California 93940		2a. REPORT SECURITY CLASSIFICATION Unclassified	
		2b. GROUP	
3. REPORT TITLE The Design and Development of a Non-Flapping Rotor System Utilizing Inflexible Blades and Employing a New Rotor Control Mechanism			
4. DESCRIPTIVE NOTES (Type of report and, inclusive dates) Engineer's Thesis; December 1972			
5. AUTHOR(S) (First name, middle initial, last name) William A. Simmons			
6. REPORT DATE December 1972		7a. TOTAL NO. OF PAGES 72	7b. NO. OF REFS 6
8. CONTRACT OR GRANT NO.		9a. ORIGINATOR'S REPORT NUMBER(S)	
9. PROJECT NO.		9b. OTHER REPORT NO(S) (Any other numbers that may be assigned this report)	
10. DISTRIBUTION STATEMENT Approved for public release; distribution unlimited.			
11. SUPPLEMENTARY NOTES		12. SPONSORING MILITARY ACTIVITY Naval Postgraduate School Monterey, California 93940	
13. ABSTRACT The intent of this study was the design, development and preliminary testing of an inflexible blade, hingeless rotor system. A hingeless system was desired due to its advantage of augmented control power resulting from its ability to transfer bending moments across the hub. The inflexible blades offered the unconventional feature of reducing the magnitude of blade flap-wise flexing to substantially zero and of removing the resultant problems of rotor dynamics. These stiffer blades generally dictated the use of more compact rotors, i.e., of a smaller diameter and therefore of a higher disk loading. The control rotor was of unconventional design and utilized a relatively small, free-flapping rotor to convey cyclic commands to the main rotor blades and provide rolling trim with varying forward speed. The present study has yielded a simple, mechanical system that essentially satisfies the design criteria and shows sufficient promise to warrant further development and testing.			



KEY WORDS	LINK A		LINK B		LINK C	
	ROLE	WT	ROLE	WT	ROLE	WT
ROTOR HEAD						
ROTOR DESIGN						
AUGMENTED FLAPPING STIFFNESS						
LIFT MOMENT DISSYMMETRY						
PURE-FEATHERING ROTOR						
PURE-FLAPPING ROTOR						
ROTOR CONTROL MECHANISM						





141755

Thesis  
S49447 Simmons  
c.1

The design and development of a non-flapping rotor system utilizing inflexible blades and employing a new rotor control mechanism.

141755

Thesis  
S49447 Simmons  
c.1

The design and development of a non-flapping rotor system utilizing inflexible blades and employing a new rotor control mechanism.

thesS49447

The design and development of a non-flap



3 2768 001 91410 4

DUDLEY KNOX LIBRARY